Neurobiology of Disease 125 (2019) 163–175

Contents lists available at ScienceDirect

Neurobiology of Disease

journal homepage: www.elsevier.com/locate/ynbdi

Mannitol decreases neocortical epileptiform activity during early brain development *via* cotransport of chloride and water

J. Glykys[a,b,*,1], E. Duquette[a], N. Rahmati[a,b], K. Duquette[a,c], K.J. Staley[a,b]

[a] Department of Neurology, Massachusetts General Hospital, Boston 02114, United States
[b] Harvard Medical School, Boston, MA 02115, United States
[c] Northeastern University, Boston 02115, United States

ARTICLE INFO

Keywords:
Development
Chloride
Cytotoxic edema
Neocortex
Water
GABA transmission
Mannitol
Seizures

ABSTRACT

Seizures and brain injury lead to water and Cl^- accumulation in neurons. The increase in intraneuronal Cl^- concentration ($[Cl^-]_i$) depolarizes the $GABA_A$ reversal potential (E_{GABA}) and worsens seizure activity. Neocortical neuronal membranes have a low water permeability due to the lack of aquaporins necessary to move free water. Instead, neurons use cotransport of ions including Cl^- to move water. Thus, increasing the extracellular osmolarity during seizures should result in an outward movement of water and salt, reducing $[Cl^-]_i$ and improving $GABA_A$ receptor-mediated inhibition. We tested the effects of hyperosmotic therapy with a clinically relevant dose of mannitol (20 mM) on epileptiform activity, spontaneous multiunit activity, spontaneous inhibitory post-synaptic currents (sIPSCs), $[Cl^-]_i$, and neuronal volume in layer IV/V of the developing neocortex of C57BL/6 and Clomeleon mice. Using electrophysiological techniques and multiphoton imaging in acute brain slices (post-natal day 7–12) and organotypic neocortical slice cultures (post-natal day 14), we observed that mannitol: 1) decreased epileptiform activity, 2) decreased neuronal volume and $[Cl^-]_i$ through CCCs, 3) decreased spontaneous multi-unit activity frequency but not amplitude, and 4) restored the anticonvulsant efficacy of the $GABA_A$ receptor modulator diazepam. Increasing extracellular osmolarity by 20 mOsm with hypertonic saline did not decrease epileptiform activity. We conclude that an increase in extracellular osmolarity by mannitol mediates the efflux of $[Cl^-]_i$ and water through CCCs, which results in a decrease in epileptiform activity and enhances benzodiazepine actions in the developing neocortex *in vitro*. Novel treatments aimed to decrease neuronal volume may concomitantly decrease $[Cl^-]_i$ and improve seizure control.

1. Introduction

The effect of the neurotransmitter GABA can be either inhibitory or excitatory depending on the relationship between the reversal potential of GABA (E_{GABA}) and the neuronal membrane potential. Values of E_{GABA} far above the neuronal membrane potential lead to excitatory actions of GABA; intermediate values of E_{GABA} lead to shunting inhibition, and values of E_{GABA} below the membrane potential result in inhibitory actions of GABA (Doyon et al., 2016; Glykys et al., 2017). E_{GABA} is mainly set by the concentration of intracellular and extracellular Cl^- with a small influence from bicarbonate, as Cl^- has a higher $GABA_AR$ permeability and concentration compared to bicarbonate (Bormann et al., 1987).

Immobile anions have been proposed to set the intraneuronal Cl^- concentration ($[Cl^-]_i$) while Cl^- co-transporters (CCCs) are key in the maintenance of this Cl^- set-point, or to return the $[Cl^-]_i$ to its baseline concentration following disruptions by synaptic transmission and/or pathological changes (Glykys et al., 2014a, 2017; for further discussion see Glykys et al., 2014b; Luhmann et al., 2014; Voipio et al., 2014). Importantly, CCCs move water besides Cl^- and cations making these cotransporters key players in the processes of regulatory volume decrease and increase observed in different cells, including neurons (Gauvain et al., 2011; Hamann et al., 2010; Lang et al., 1998; MacAulay and Zeuthen, 2010; Zeuthen, 1991; Zeuthen and Macaulay, 2012).

High neuronal $[Cl^-]_i$ is observed in different brain regions, including the neocortex, during early brain development (Ben-Ari et al., 2007; Glykys and Staley, 2016; Sulis Sato et al., 2017) and results in depolarizing actions of GABA (Glykys et al., 2009; Kirmse et al., 2015; Rheims et al., 2008). Elevated neuronal $[Cl^-]_i$ is also observed in pathological conditions including gliomas (Pallud et al., 2014), during

* Corresponding author at: Department of Pediatrics, Iowa Neuroscience Institute, Carver College of Medicine, University of Iowa, Iowa City 52242, United States.
E-mail address: joseph-glykys@uiowa.edu (J. Glykys).
[1] *Current corresponding address:* Department of Pediatrics, Iowa Neuroscience Institute, Carver College of Medicine, University of Iowa, Iowa City, 52242.

https://doi.org/10.1016/j.nbd.2019.01.024
Received 21 August 2018; Received in revised form 28 January 2019; Accepted 30 January 2019
Available online 01 February 2019
0969-9961/

reperfusion after oxygen-glucose deprivation (Blauwblomme et al., 2018; Pond et al., 2006), and seizures (Dzhala et al., 2010; Glykys et al., 2009; Huberfeld et al., 2007). Importantly, high neuronal $[Cl^-]_i$ contributes to anticonvulsant inefficacy during neonatal seizures (Dzhala et al., 2005; Glykys et al., 2009; Glykys and Staley, 2015; Mazarati et al., 2009; Nardou et al., 2011b), a condition which is difficult to treat in humans (Glass, 2014; Painter et al., 1999; Stevenson et al., 2016).

Cytotoxic edema is caused by neuronal water shifts coupled with ionic movements, especially of Cl^- (Allen et al., 2004; Dijkstra et al., 2016; Rungta et al., 2015), and it is observed in different neurological conditions including traumatic brain injury, seizures and ischemia (Glykys et al., 2017). Mannitol and hypertonic saline are used frequently in clinical practice to treat increased intracranial pressure which is a consequence of severe cytotoxic and vascular edema (Carney et al., 2016; Ropper, 2014). These osmotic agents are thought to lead to the movement of pure water out of cells. Here we test whether mannitol leads to the exit of pure water out of neocortical neurons, or if there is a link between water and Cl^- outward movement, as neuronal membranes have a low water permeability (Aitken et al., 1998; Andrew et al., 2007; Caspi et al., 2009) due to a lack of aquaporins that are present in other cells (Lang et al., 1998). If linked, mannitol should decrease $[Cl^-]_i$, make E_{GABA} more negative, and improve GABAergic anticonvulsant efficacy. However, if water and $[Cl^-]_i$ movement are unlinked, hypertonic therapies should draw pure water out of the cytoplasm. This would increase $[Cl^-]_i$, make E_{GABA} more positive and decrease the effectiveness of GABAergic anticonvulsants.

2. Materials and methods

2.1. Animals

Postnatal CLM-1 Clomeleon (P7–14; C57bl/6 background, gift from G. Augustine) and C57bl/6 (WT, P7–63; RRID:IMSR_JAX:000664) mice of both sexes were anesthetized using inhaled isoflurane and decapitated per protocol, approved by the Institutional Animal Care and Use Committee of the Massachusetts General Hospital Center for Comparative Medicine. The brain was removed and placed in ice-cold artificial cerebrospinal fluid (aCSF) containing (in mM) NaCl (120), KCl (3.3), $CaCl_2$ (1.3), $MgCl_2$ (2), NaH_2PO_4 (1.25), $NaHCO_3$ (25), and D-glucose (10) with pH 7.3–7.4 when bubbled with 95% O_2 and 5% CO_2 (287 ± 4 mOsm, $n = 9$; mean ± SD). Coronal brain slices, 350–500 μm thick, were cut using a vibratome (Leica VT1000S) while submerged in aCSF containing 2 mM kynurenic acid. The brain slices were placed in an interface holding chamber containing aCSF (1.3 mM $MgCl_2$) at room temperature for 30 min. Next, the temperature was slowly increased and held at 30 °C. Slices were stored for 1 h minimum before being transferred to the recording chamber. For some imaging experiments the slices were incubated in Low-Mg^{2+} aCSF for at least 1 h. *Organotypic slices*: P6–7 coronal 400 μm thick neocortical slices (frontal region, pre-hippocampus) were cut using a McIlwain tissue chopper. Slices were mounted in clots of chicken plasma and thrombin on poly-L-lysine-coated glass coverslips. Slices were incubated in roller tubes at 36 °C with 750 μL of Neurobasal A/B27 medium supplemented with 0.5 mM GlutaMAX, 30 μg/ml gentamicin, and 20 mM NaCl to reach a final media osmolarity of 279 ± 6 mOsm ($n = 11$; mean ± SD). The culture media was changed bi-weekly.

2.2. Imaging

Two-photon imaging was performed using a Fluoview 1000MPE two-photon microscope with pre-chirp optics and a fast acoustic-optical modulator mounted on an Olympus BX61WI upright microscope body with a 25× water immersion objective (NA 1.05). A Ti:sapphire mode-locked laser (DeepSee Mai Tai; Spectra-Physics) generated two-photon fluorescence with 860 nm excitation. Emitted light was bandpass filtered through two emission filters: 460–500 nm for cyan fluorescence protein (CFP) and 520–560 nm for yellow fluorescence protein (YFP). Two photomultiplier tubes (Hamamatsu Photonics) were used to simultaneously acquire CFP and YFP signals. Slices were perfused with Low-Mg^{2+} aCSF, held at 32-34 °C and aerated with 95% O_2–5% CO_2. Three-dimensional stacks (3D) of raster scans in the XY plane (282.072 μm × 282.072 μm) were imaged at a z-axis interval of 2 μm, resolution 512 × 512 pixels.

2.3. Neuronal Cl^- determination

Quantitative measurements of neuronal $[Cl^-]_i$ and area of 3D stacks were performed using ImageJ (National Institutes of Health, RRID:SCR_003070) as described previously (Glykys et al., 2009) with modifications for area determination. The CFP and YFP z-stack images were loaded and the corresponding background level was subtracted from the entire 3D stack. Next, 3D planes were median filtered. Maximum intensity *Z*-projections were created every 10 μm for neuronal area determination. This allowed us to have, in a single plane, the maximal area (MaxArea) projection for each neuron. A region of interest (ROI) was drawn manually around the cell bodies (MaxArea) based on an automatic neuronal edge detection plugin in ImageJ (Canny Edge Detector plugin, Fig. 3A). The ratio of the YFP/CFP fluorescence intensity was obtained for each pixel in the ROI at the z-plane corresponding to the MaxArea. Next, the median YFP/CFP ratio of the ROI was calculated. The following equation converted each cell's YFP/CFP ratio into $[Cl^-]_i$:

$$[Cl^-]_i = K'_D \frac{(R_{max} - R)}{(R - R_{min})} \quad (1)$$

where K'_D is the apparent dissociation constant, R_{max} is the ratio when Clomeleon is not bound to Cl^-, and R_{min} is when Clomeleon is completely quenched. The following values were used: K'_D of 91 mM, R_{max} of 1.026, and R_{min} of 0.268 based on our calibrations (Glykys et al., 2014a, 2009). Recalibration in 2016 did not show significant difference in these values: $K'_D = 81.47$ mM, $R_{max} = 1.026$, $R_{min} = 0.244$. The median $[Cl^-]_i$ was used as its distribution is skewed to lower values (non-Gaussian distribution). Cells with $[Cl^-]_i$ above 130 mM were excluded from analysis (5% of imaged cells).

2.4. Electrophysiology

Acute brain slices were placed in an upright microscope (Zeiss, Axioskop) or a custom-made interphase chamber and perfused with aCSF containing 0 mM $MgCl_2$ (Low-Mg^{2+}) to induce epileptiform activity. They were held at 32–34 °C and aerated with 95% O_2–5% CO_2 (flow rate of 5–8 ml/min). Glass electrodes were placed in neocortex layer IV/V and extracellular field potentials were recorded using a low-noise multichannel amplifier (EX 4–400, Dagan Corporation) with a 1000× gain and digitized at 2 kHz using an analog to digital converter (DigiData 1321A, Molecular Devices). Analysis was performed using a custom-written macro in IgorPro v6.35 (Wavemetrics, RRID:SCR_000325) as previously described (Glykys et al., 2009). For each 30-s epoch, the mean value was subtracted and Fast Fourier Transformed (FFT) was obtained using a Hanning window apodization. The FFT (30,000 points) was smoothed using a running-median window of seven points, divided by the total number of points, and the signal area (1–500 Hz) was calculated (wide-band power). Finally, the mean FFT power during equal baseline and drug condition epochs was calculated. Tungsten electrodes were used to record multiunit activity (MUA). Recordings were high-pass filtered at 10 Hz and events were detected in Clampfit (Molecular Devices). Drug effects were compared between epochs prior to the drug perfusion, at the end of the drug perfusion, and at the end of washout. *Pyramidal cell recordings:* Layer IV/V pyramidal cells were recorded in regular aCSF in whole-cell voltage-clamp mode using pipettes filled with (in mM) 140 CsCl, 4 NaCl, 0.5 $CaCl_2$, 10 HEPES, 5 EGTA and 2 MgATP. Ionotropic glutamate

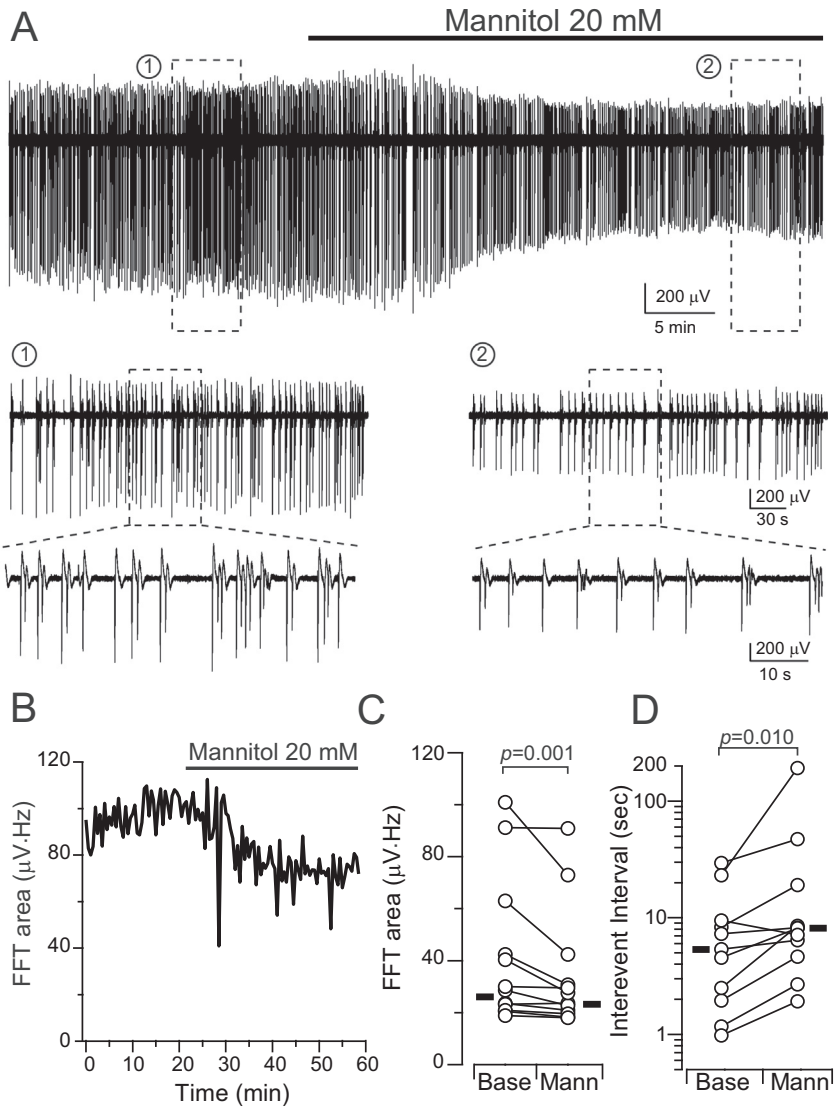

Fig. 1. A clinical dose of mannitol decreases neocortical epileptiform activity in acute neocortical slices during early brain development. A) *Top*, *in vitro* epileptiform activity induced by Low-Mg^{2+} in the neocortex (P8, acute brain slice, Layer IV/V) recorded with extracellular electrodes. Mannitol (20 mM) perfusion shown by line. *Middle*, higher magnification of boxed segments from baseline (1) and during mannitol perfusion (2). *Below*, further magnification of box segments. B) FFT area from trace in A calculated every 30 s. C) Mannitol anticonvulsive effect, P7–12 (open circles: individual recordings; thick line: median; $n = 12$, Wilcoxon Signed Rank Test; Log scale). D) Interevent interval change during mannitol application (line: median; $n = 11$, Wilcoxon Signed Rank Test).

receptors were blocked with 2 mM kynurenic acid. Spontaneous inhibitory post-synaptic currents (sIPSCs) were recorded at baseline and followed by application of 20 mM mannitol at room temperature (holding potential of −75 mV). Signal acquisition was performed using a Multiclamp amplifier (Multiclamp 700B; Molecular Devices) with Clamplex 10 software (Molecular Devices). Signals were sampled at 10 KHz and analyzed using Clampfit program (Clampfit 10.6, Molecular Devices).

2.5. Experimental design and statistical analysis

$[Cl^-]_i$ was expressed as a median and an interquartile range (IQR), as $[Cl^-]_i$ follows a non-Gaussian distribution. Gaussian distribution of data was tested with the Shapiro-Wilk test. Paired and unpaired *t*-tests were used for parametric comparisons (2 conditions). The Wilcoxon Signed Rank Test (WSRT) was used for non-parametric paired data. One-way repeated analysis of variance (ANOVA) was used for multiple comparisons of parametric data with Holm-Sidak post-hoc test. Friedman Repeated ANOVA and Kruskal-Wallis One Way ANOVA on Ranks were used for multiple comparisons of non-parametric data with Tukey post-hoc test. Kolmogorov-Smirnov test was performed to test the peak cumulative distributions of MUA. Statistical significance was set to $p < .05$. IgorPro v6.35 (Wavemetrics, RRID:SCR_000325) and SigmaPlot v.11 (Systat Software, Inc., RRID:SCR_003210) were used for data analysis.

2.6. Reagents and solution osmolarity

Mannitol (two different batches including one with 99.9999% purity), kynurenic acid, 4-aminopyridine, diazepam and furosemide were all obtained from Sigma-Aldrich. Solution osmolarity was measured with a vapor pressure osmometer (Vapro 5520, Wescor Inc) calibrated each day a measurement was made. Osmolarity of the aCSF used for incubation and recordings was 289 ± 6 mOsm ($n = 16$; mean ± SD). The organotypic slice incubation solution had an osmolarity of 290 ± 2 mOsm ($n = 4$; mean ± SD) on experiment day (when slices were removed from roller tubes and placed in the recording chamber). Slices equilibrated in aCSF for at least 10 min prior to an experimental recording. Changes in aCSF osmolarity by mannitol or hypertonic saline were verified by vapor pressure osmometer (Control: 289 ± 6; Hyperosmolar solution: 310 ± 6 mOsm, $n = 16$; mean ± SD).

3. Results

3.1. A clinical dose of mannitol decreases neocortical epileptiform activity during early neocortical development

Mannitol increases extracellular osmolarity, decreases cell swelling, and is used to treat increased intracranial pressure in clinical practice (Bratton et al., 2007; Pitfield et al., 2012). Neurons do not have aquaporins to move free water (Amiry-Moghaddam and Ottersen, 2003) and have a low water permeability (Aitken et al., 1998; Andrew et al., 2007; Caspi et al., 2009; Lang et al., 1998; Risher et al., 2009). Instead, water shifts are associated with ionic movement including Cl^- (Hoffmann et al., 2009; Jourdain et al., 2011; Lambert et al., 2008; Rungta et al., 2015; Zeuthen, 2010). We hypothesized that a reduction in neuronal volume, due to mannitol perfusion, will lead to a concomitant reduction in neuronal $[Cl^-]_i$. This reduction in $[Cl^-]_i$ should enhance inhibitory actions of GABA and decrease epileptiform activity if present.

First, we determined if the addition of 20 mM mannitol to the aCSF leads to a decrease of epileptiform activity in neocortical brain slices during early brain development (P7–12) when GABA has excitatory actions (Glykys et al., 2009; Rheims et al., 2008). This mannitol dose increases the aCSF osmolarity by 20 mOsm, which corresponds to the change obtained by a clinically relevant dose of mannitol (1 g/kg) commonly used in pediatric and adult populations for the treatment of increased intracranial pressure (Cloyd et al., 1985; Marshall et al., 1978; Polderman et al., 2003).

In vitro epileptiform activity in neocortical brain slices (Layer IV/V) of P7–12 WT mice was induced by Low-Mg^{2+} (Mody et al., 1987) and measured by field electrodes. Mannitol (20 mM) was perfused after a baseline period (Fig. 1A), and epileptiform activity was measured by FFT power for equal time periods of baseline and drug application (Fig. 1B). Mannitol perfusion led to a 14% decrease (SD = 13) in epileptiform activity from 29.3 μV*Hz (interquartile range, IQR = 22.1–52.7) to 25.6 μV*Hz (IQR = 20.2–36.5; $n = 12$, $p = .001$, WSRT; Fig. 1C). The inter-event interval increased in the presence of mannitol from 5.4 s (IQR = 2.1–9.2) to 8.2 s (IQR = 5.1–16.5; $n = 11$, $p = .01$, WSRT; Fig. 1D). To test reproducibility, we repeated this experiment using a different batch of mannitol and obtained the same decrease in epileptiform activity (29.3 μV*Hz [IQR = 23.4–30.8] to 20.8 μV*Hz IQR 20.3–26.9; $n = 7$, $p = .016$ WSRT; 15% decrease [SD = 12]).

We further verified the effect of mannitol on neocortical epileptiform activity in a different *in vitro* model, the neocortical organotypic slice culture. The organotypic preparation develops spontaneous epileptiform activity in regular aCSF (Glykys and Staley, 2015) with the advantage of not requiring the addition of pro-convulsive chemicals or altering its ionic composition. We recorded and analyzed epileptiform activity using the same methods as in acute brain slices. Like the effect observed in the Low-Mg^{2+} model, 20 mM mannitol perfused in regular aCSF (1.3 mM $MgCl_2$) produced a significant reduction in epileptiform activity at days *in vitro* 7–8 (DIV) from 28.9 μV*Hz (IQR = 23.7–37.1) to 24.5 μV*Hz (IQR = 21–30.2; $n = 9$, $p = .004$, WSRT; Fig. 2A-C) corresponding to a 16% decline (SD = 7). Mannitol produced a similar decrease in epileptiform activity in a subgroup of experiments where a washout was performed (Baseline: 26.1 ± 4.64 μV*Hz; Mann: 22.3 ± 3.50 μV*Hz; Washout: 26 ± 5.27 μV*Hz; $n = 6$, $F(2,10) = 10.05$, $p = .004$, One-way repeated ANOVA; Holm-Sidak post-hoc test significant between Baseline *vs.* Mann and between Mann *vs.* Wash, $p = .003$). There was no difference in the mannitol effect on epileptiform activity between acute and organotypic slices ($p = .769$, unpaired *t*-test; Fig. 2D). The epileptiform activity amplitude decrease during mannitol perfusion was not due to a reduction in extracellular space resistance (field effect; Jefferys, 1995) as mannitol did not lead to a fall in multi-unit activity amplitude in the absence of seizures (see below). Therefore, the change in epileptiform amplitude represents a decrease in neuronal recruitment.

These results indicate that an increase in the extracellular osmolarity with a clinically relevant dose of mannitol leads to a decrease in neocortical epileptiform activity during early brain development in both an induced and a spontaneous seizure model.

3.2. Mannitol reduces neuronal volume and $[Cl^-]_i$ in neurons with high initial $[Cl^-]_i$

Neuronal $[Cl^-]_i$ increases during neonatal seizures (Glykys et al., 2009), it gradually decreases after seizure termination (Dzhala et al., 2010; Glykys et al., 2009; Nardou et al., 2011b), and the rise in $[Cl^-]_i$ is associated with an increase in neuronal volume (Glykys et al., 2014a). Therefore, we evaluated whether the decrease in epileptiform activity mediated by mannitol correlates with a reduction in neuronal volume and $[Cl^-]_i$. We quantified neuronal $[Cl^-]_i$ using Clomeleon mice which express a genetically encoded ratiometric Cl^- sensitive fluorophore (Kuner and Augustine, 2000). It has the advantage of assessing the neuronal $[Cl^-]_i$ directly and simultaneously from many neurons. Neuronal volume (using the maximal neuronal area [MaxArea], see methods) and $[Cl^-]_i$ were measured by multiphoton imaging in the neocortical layer IV/V of acute brain slices (P11–12) exposed to Low-Mg^{2+} aCSF followed by a 20 mM mannitol perfusion (Fig. 3A). Slices exposed to Low-Mg^{2+} aCSF resulted in high $[Cl^-]_i$ (Fig. 3A,B; Supplemental Fig. 1) as previously observed (Dzhala et al., 2012, 2010, Glykys et al., 2014a, 2009).

Neuronal $[Cl^-]_i$ decreased in neocortical layer IV/V neurons from 28.4 mM (IQR:19–50.4) to 24.2 mM (IQR: 14.6–43.6) after 5 min of mannitol perfusion and to 19.0 mM after 20 min of mannitol (IQR: 10.5–30.8) ($p < .001$, Friedman Repeated measures ANOVA on Ranks; significance between the 3 conditions, $p < .05$ post-hoc Tukey test; Fig. 3B). This change in $[Cl^-]_i$ corresponds to a change in E_{Cl} from −39 to −49 mV (Nernst equation calculation). MaxArea also decreased after 5 min of mannitol perfusion from 254 μm^2 (IQR: 179–312) to 245 μm^2 (IQR: 183–293) and to 226 μm^2 after 20 min (IQR: 176–297; $n = 107$ paired neurons, 5 slices, $p < .001$ Friedman Repeated ANOVA on Ranks; significance between initial condition and both mannitol perfusion at 5′ and 20′, $p < .05$ post-hoc Tukey test, Fig. 3B). Notably, neurons with the highest initial $[Cl^-]_i$ had the greatest decrease under mannitol ($R^2 = 0.085$ at 5′, $p = .002$; and $R^2 = 0.395$ at 20′, $p < .001$; Fig. 3C). This is in contrast with the decrease of MaxArea by mannitol which is independent of the initial neuronal area ($p > .05$ at 5′ and 20′, Fig. 3D) due to the large variance of neuronal sizes. Notably, neurons that had a high initial $[Cl^-]_i$ had a larger decrease in MaxArea ($R^2 = 0.085$ at 5′, $p = .002$ and $R^2 = 0.104$ at 20′, $p < .001$; Fig. 3E). A correlation was observed between the change in $[Cl^-]_i$ and neuronal MaxArea at 20 min ($R^2 = 0.088$, $p = .002$, Fig. 3F) but no significant difference was observed at 5 min ($p = .198$). Neurons exposed to only Low-Mg^{2+} aCSF and no mannitol maintained a stable $[Cl^-]_i$ and MaxArea for up to 30 min of sequential measurement (Supplemental Fig. 1).

Next, we addressed whether CCCs are involved in the co-transport of water and Cl^- during epileptiform activity induced by Low-Mg^{2+}. CCCs were blocked with furosemide 300 μM (Pond et al., 2006) as higher doses of this drug can lead to a significant block of NMDA receptors (Lerma and Martin del, 1992). Perfusion of mannitol in the presence of furosemide resulted in a small but significant increase in $[Cl^-]_i$ (Fig. 4, $p \leq .001$; Friedman Repeated ANOVA on Ranks, $p < .05$ by Tukey post-hoc test between furosemide and furosemide + mannitol). Mannitol was still able to decrease MaxArea in the presence of furosemide (Fig. 4, $p = .003$; Friedman Repeated ANOVA on Ranks, $p < .05$ by Tukey post-hoc test between furosemide and furosemide + mannitol). These observations indicate that when CCCs are blocked, co-transport of water and Cl^- become unlinked so that an increase in extracellular osmolarity induced by mannitol results in a net loss of free water and leads to an increase in intracellular Cl^-. The decrease in neuronal MaxArea when CCCs are blocked suggests that water can

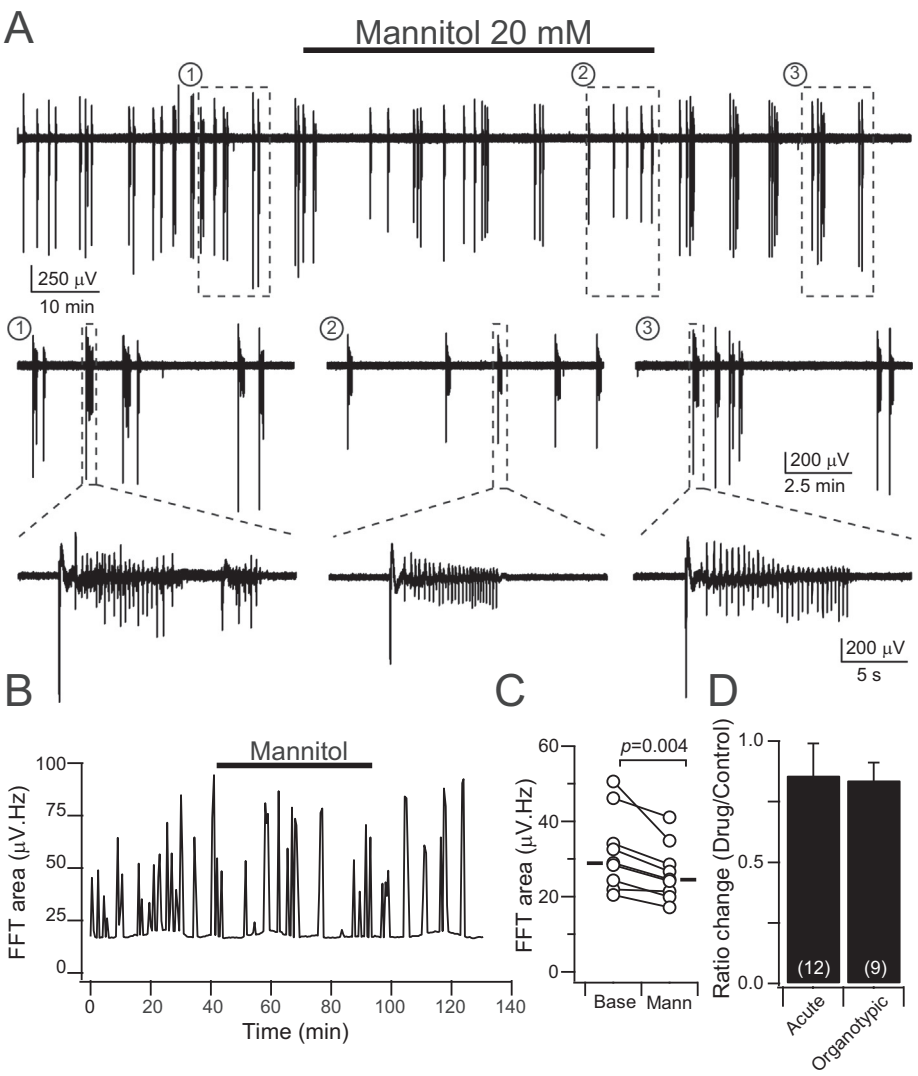

Fig. 2. A clinical dose of mannitol decreases neocortical epileptiform activity in neocortical organotypic slice cultures. A) *Top*, epileptiform activity recorded in a neocortical organotypic slice culture (DIV8, Layer IV/V) in the presence of regular aCSF and mannitol. *Below*, higher magnification of baseline (1), during mannitol perfusion (2), and washout (3). B) FFT area from trace in A calculated every 60 s. C) Mannitol anticonvulsive effect, pooled data (open circles: individual recordings; thick line: median; $n = 9$, Wilcoxon Signed Rank Test). D) Effect of mannitol on epileptiform activity between acute and organotypic slices (mean ± SD; $p = .769$, unpaired *t*-test).

escape through other non-CCC pathways (MacAulay and Zeuthen, 2010). However, when CCCs are operative, the water and Cl^- responses are determined by CCC activity. Together, these results indicate that the action of mannitol on epileptiform activity correlates with a concomitant decrease in neuronal MaxArea and $[Cl^-]_i$ mediated primarily by CCCs, especially in neurons with high initial $[Cl^-]_i$.

3.3. Mannitol reduces spontaneous multiunit activity frequency but not amplitude

Next, we verified the functional changes in $[Cl^-]_i$ using a Cl^- imaging independent technique. We measured MUA in the neocortex (layer IV/V) of acute brain slices (P7–8) in the presence of 50 μM 4-aminopyridine (to increase the frequency of action potentials) plus 2–3 mM kynurenic acid (glutamatergic excitatory transmission blocker) to determine if a decrease in $[Cl^-]_i$ by mannitol causes a reduction in action potential firing as a result of an increase in GABAergic inhibition (Fig. 5A). These experiments also address if the decrease in epileptiform activity amplitude, observed in the presence of mannitol (Figs. 1 and 2), is due to a decrease in extracellular conductivity (Jefferys, 1995). MUA, as an assay of extracellular conductivity, is independent of the summation of ligand- and voltage-gated membrane currents. Mannitol perfusion (20 mM) produced a significant decrease in spontaneous MUA frequency from 2.08 Hz (IQR 0.42–2.66) to 1.10 Hz (IQR: 0.24–1.76) between 5 and 10 min and to 0.49 Hz (IQR: 0.08–1.39) between 10 and 15 min ($n = 12$, $p < .001$, Friedman Repeated ANOVA on Ranks, difference between baseline and both conditions $p < .05$, Tukey post-hoc test Fig. 5B, F). These results indicate that mannitol enhanced the inhibitory effect of spontaneously released GABA in brain slices as excitatory transmission is blocked by kynurenic acid. It is also an independent confirmation of the $[Cl^-]_i$ decrease observed with Clomeleon imaging. We did not find evidence that this concentration of mannitol in the developing neocortex decreased the extracellular conductivity (field effect) because there was no change in MUA peak amplitudes (Baseline: 21.8 μV [IQR: 18.8–26.3], Mann 5–10 min 20.4 μV [18.5–26-6], Mann 10–15 min 21.3 μV [17.6–25.2], $p = .472$ Friedman Repeated ANOVA on Ranks; Fig. 5C-E) nor a change in baseline root mean square noise (Baseline: 3.14 μV [IQR: 3.08–3.25], Mann 5–10 min 3.15 μV [3.06–3.2], Mann 10–15 min 3.12 μV [3.03–3.25], $p = .338$ Friedman Repeated ANOVA on Ranks; Fig. 5G).

While it is unlikely that 20 mM mannitol can induce a change in the GABA release probability as one order of magnitude higher concentrations of sugars are needed (500 mM *vs.* 20 mM; Bekkers and Stevens, 1996; Staley et al., 1998; Stevens and Tsujimoto, 1995) we decided to test this possibility. Indeed, we observed no change in the frequency nor amplitude of sIPSCs recorded in layer IV/V neocortical neurons during whole cell voltage clamp experiments where the neuronal $[Cl^-]_i$ closely matches the pipette's $[Cl^-]_i$ (Sup. Fig. 2).

This data, combined with our Cl^- imaging, strongly indicates that a clinical dose of mannitol decreases neuronal $[Cl^-]_i$ leading to a more

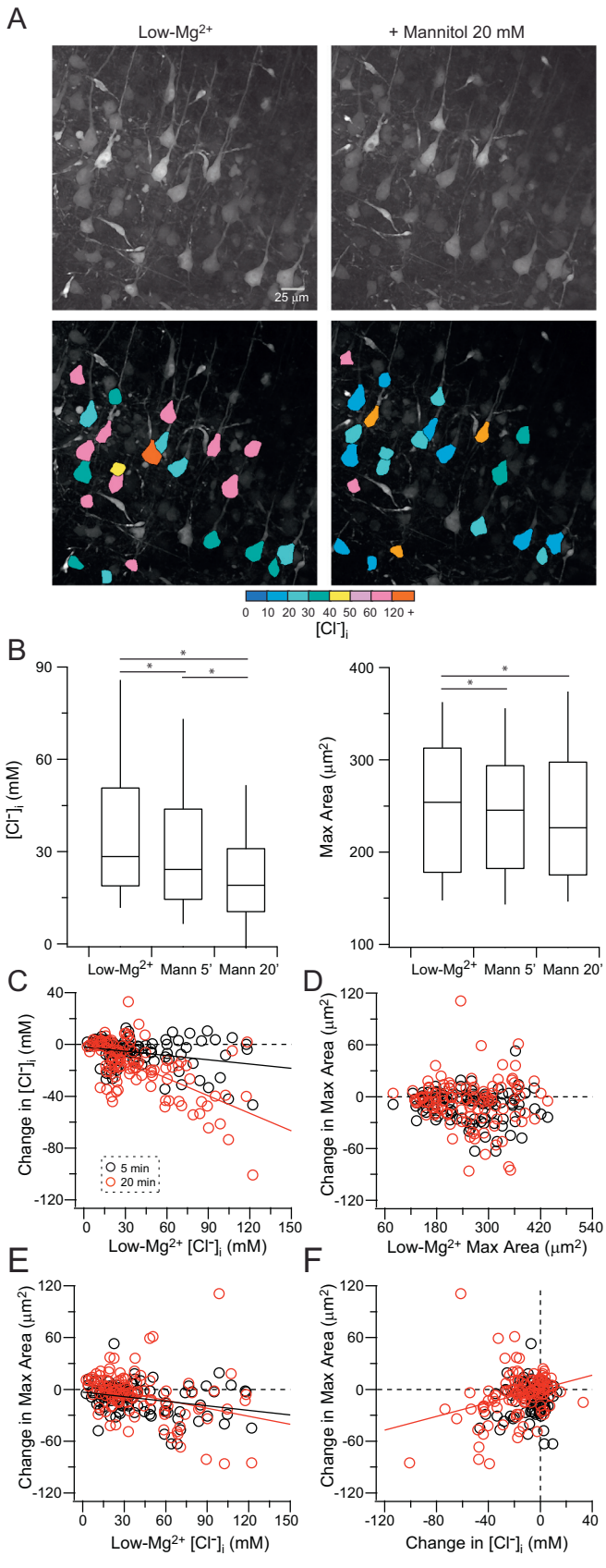

Fig. 3. Mannitol reduces neuronal volume and $[Cl^-]_i$ in neurons with high initial $[Cl^-]_i$. A) *Top*, Two-photon stack image (CFP) of a P10 neocortical slice (Layer IV/V) expressing Clomeleon during Low-Mg^{2+} (left) and after 20 min of mannitol perfusion (right). Contrast, brightness, gamma identical between both images. *Below*, ROI of neurons that completed the treatment. $[Cl^-]_i$ is pseudo-colored. B) The neuronal $[Cl^-]_i$ (*left*) and maximal area (MaxArea, *right*) decreased during mannitol perfusion ($n = 107$ paired neurons, 5 slices, $p < .001$ Friedman Repeated ANOVA on Ranks, * is $p < .05$ by Tukey post-hoc test). C) Correlation between baseline $[Cl^-]_i$ and its change after mannitol perfusion. Line stands for linear regressions ($R^2 = 0.085$ at 5′, $p = .002$; and $R^2 = 0.395$ at 20′, $p < .001$). D) No correlation between baseline neuronal MaxArea and its change after mannitol perfusion. E) Correlation between baseline $[Cl^-]_i$ and the change in MaxArea ($R^2 = 0.085$ at 5′, $p = .002$ and $R^2 = 0.104$ at 20′, $p < .001$). F) Significant correlation between the change in neuronal MaxArea and $[Cl^-]_i$ after 20 min of mannitol ($R^2 = 0.088$, $p = .002$).

efficacious inhibitory effect of endogenous GABA.

3.4. A decrease in neuronal $[Cl^-]_i$ by mannitol potentiates the effect of benzodiazepines during early neocortical development but not at older ages

A clinical dose of mannitol decreased neuronal $[Cl^-]_i$ and produced a significant reduction in epileptiform activity (Figs. 1–3). Next, we explored whether this dose of mannitol enhances the anticonvulsive action of a clinically relevant dose of diazepam ($GABA_AR$ positive allosteric modulator), that by itself is not effective during early neocortical development (Connell et al., 1989; Glykys and Staley, 2015; Nardou et al., 2011a). We tested 0.5 µM of diazepam which corresponds to a concentration of 0.14 mg/L. A drug plasma concentration of 0.15 mg/L (range: 0.07–0.23 mg/L) is found in human neonates after receiving diazepam at an anticonvulsant dose of 0.1–0.3 mg/kg, using a volume of distribution of 1.3 L/kg (Anderson and Miller, 2002; Greenblatt and Sethy, 1990).

We recorded *in vitro* epileptiform activity induced by Low-Mg^{2+} using field electrodes in the neocortex layer IV/V of P10–11 mice. We assessed the effect of diazepam (0.5 µM; DZP) followed by the addition of 20 mM mannitol (Mann + Dzp). Mann + Dzp significantly decreased epileptiform activity but diazepam alone did not (Baseline: 37 ± 6.45 µV*Hz, Dzp 32.2 ± 9.21 µV*Hz, Mann + Dzp 24.6 ± 5.15 µV*Hz; $n = 8$, $F(2,14) = 9.409$, $p = .003$, One-way repeated ANOVA, significance between Mann + Dzp and Baseline and between Mann + Dzp and Dzp, $p < .001$and $p = .019$ respectively, Holm-Sidak post-hoc test; Fig. 6A-C). Also, the ratio effect of Mann + Dzp is significantly greater than mannitol alone (Mann: 0.89 IQR: 0.72–0.97, $n = 12$; Mann + Dzp: 0.69 IQR: 0.5–0.84, $n = 8$; $p = .041$, Mann-Whitney Rank Sum Test; Fig. 6D). The ineffectiveness of diazepam at this age is consistent with prior publications in the organotypic neocortical slice cultures (Glykys and Staley, 2015), in cultured hippocampal neurons and in the intact hippocampus (Deeb et al., 2013; Nardou et al., 2011a). In contrast, the same dose of diazepam (0.5 µM) decreased epileptiform activity in adult (P31–63) neocortical brain slices (9/9 slices), but it was not enhanced by mannitol (Baseline: 27.7 ± 0.88 µV*Hz, Dzp: 24.5 ± 6.73 µV*Hz, Man + Dzp: 23.3 ± 5.96 µV*Hz, Washout: 25.7 ± 8.15 µV*Hz; $n = 9$, $F(3,24) = 7.07$, $p = .001$, one-way repeated ANOVA; significant between Baseline and both Dzp and Man + Dzp $p < .001$ and $p = .004$ respectively, Holm-Sidak post-hoc test; Fig. 6F, G).

These results indicate that an ineffective dose of diazepam can become effective when $[Cl^-]_i$ is lowered by mannitol during early brain development. In contrast, as adult neuronal $[Cl^-]_i$ is already lower than during early brain development (Glykys et al., 2009; Glykys and Staley, 2016; Owens et al., 1996; Rheims et al., 2008; Sulis Sato et al., 2017), a clinical dose of diazepam is already effective and mannitol cannot further enhance it. These results also agree with our prior data in which a clinical dose of diazepam is ineffective when the baseline neuronal $[Cl^-]_i$ is high but is effective when $[Cl^-]_i$ is low (Glykys and Staley,

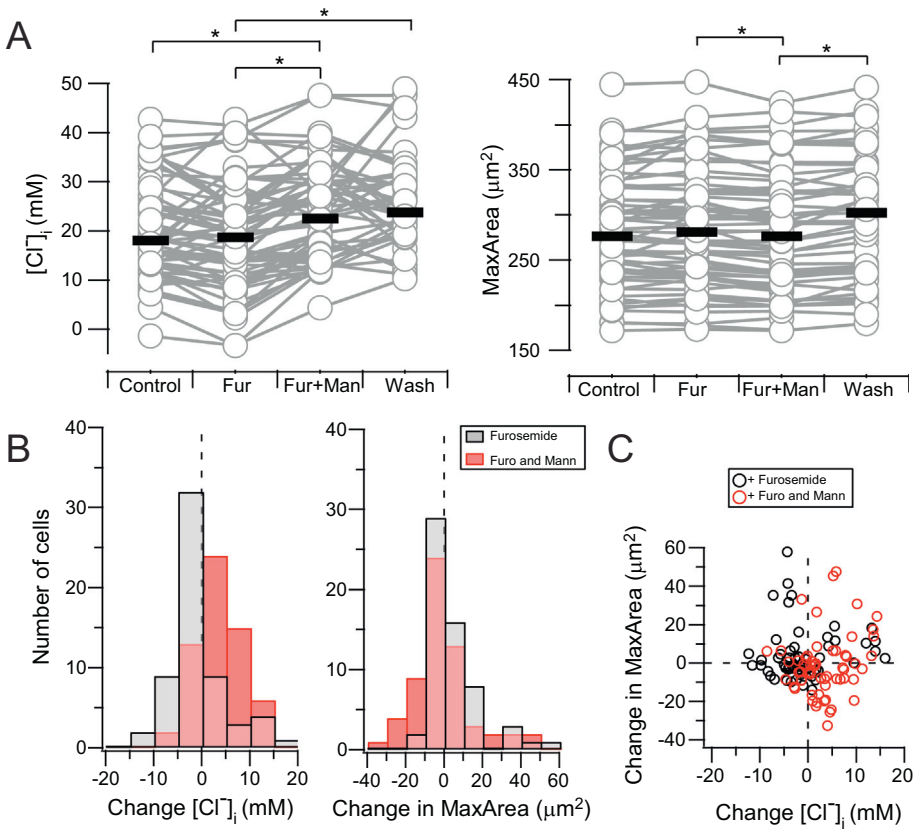

Fig. 4. Blocking CCCs prevent the decrease of $[Cl^-]_i$ and volume by mannitol. A) Neuronal $[Cl^-]_i$ (left) and MaxArea (right) measured with 2-photon imaging of Clomeleon expressing Layer IV/V neocortical neurons (P9–12) under Low-Mg^{2+} after sequential perfusion of furosemide (Fur), furosemide + mannitol (Fur + Man) and washout (Wash). Six slices, $n = 60$ paired neurons, Friedman Repeated ANOVA on Ranks, $p < .001$ for $[Cl^-]_i$ and $p = .003$ for MaxArea. * is $p < .05$ by Tukey post-hoc test. ($[Cl^-]_i$ in mM: Control 18.1 [IQR:13.2–26], Fur: 18.8 [11–25.4], Fur + Man 22.6 [15.1–30.2], Wash 23.8 [19.4–31.3]. MaxArea in μm: Control 277 [237–331], Fur 281 [233–328], Fur + Man 277 [227–326], Wash 303 [239–352]). B) Absolute change in $[Cl^-]_i$ (left) and MaxArea (right) in the presence of drugs in A. C) Combined change in $[Cl^-]_i$ and MaxArea in the presence of drugs in A.

2015). The ineffectiveness of mannitol in the adult neocortex could be due to a lower number of neurons with high $[Cl^-]_i$ compared to the neonatal brain (Glykys et al., 2009) or by the re-establishment of low $[Cl^-]_i$ after seizures by CCCs, mainly K^+-Cl^- cotransporters (Moore et al., 2017).

Finally, hypertonic saline is another clinical therapy often used to treat increased intracranial pressure. We studied if adding an additional 10 mM of NaCl to the aCSF (a similar 20 mOsm increase as produced with 20 mM mannitol) would also result in a decrease in neocortical epileptiform activity. Hypertonic saline did not decrease epileptiform activity in acute neocortical brain slices (P9–13) exposed to Low-Mg^{2+}. The same recording and analysis methods were used as before (Baseline: 60.9 ± 2.05 μV*Hz, +NaCl: 63.1 ± 2.45 μV*Hz, $n = 12$, $p = .814$, paired t-test). The ineffectiveness of increasing the extracellular osmolarity by a higher concentration of extracellular NaCl may be due to an enhanced neuronal import of Cl^- by the Na^+- K^+-Cl^- co-transporter (NKCC1); however, this was outside the scope of our present study.

4. Discussion

4.1. Summary

Our results performed in the neocortex show: 1) A clinical concentration of mannitol decreases neocortical epileptiform activity during early brain development in two different seizure models. 2) The anticonvulsant effect of mannitol is associated with a decrease in neuronal volume and $[Cl^-]_i$ in neurons with high initial $[Cl^-]_i$. 3) The linked movement of water and Cl^- out of neurons is mediated primarily by CCCs. 4) Mannitol leads to a decrease in MUA frequency but not amplitude. 4) Mannitol potentiates the effect of a clinical dose of diazepam on neocortical epileptiform activity during early brain development, and 5) a similar increase in aCSF osmolarity by NaCl did not reduce epileptiform activity. We conclude that enhancing the outflux of water in neurons with pathologically elevated $[Cl^-]_i$ results in reduced neuronal volume and $[Cl^-]_i$, decreased epileptiform activity, and enhanced actions of positive allosteric $GABA_A$Rs modulators (Fig. 7). These results are not consistent with the independent movement of water and Cl^- across neuronal membranes because: 1) neurons have a low water membrane permeability (Aitken et al., 1998; Andrew et al., 2007; Caspi et al., 2009; Lang et al., 1998); and 2) increased extracellular osmolarity would have drawn pure water out of the neuronal cytoplasm, raising the neuronal $[Cl^-]_i$ (with no need for dissipation of the increased $[Cl^-]_i$ because neurons can sustain elevated levels in physiological and pathological conditions, Ben-Ari, 2002; Huberfeld et al., 2007; Pond et al., 2006) and further compromising GABAergic inhibition.

4.1.1. Neuronal Cl^- and volume

There is a positive correlation between $[Cl^-]_i$ and neuronal swelling. Neuronal swelling (Caspi et al., 2009; Glykys et al., 2009, 2014a; Steffensen et al., 2015) can arise by changes in the ionic concentration (especially for K^+ and Cl^-) and changes in the extracellular space that happen during prolonged neuronal activity and seizures (Dietzel et al., 1980, 1982, 1989; Dzhala et al., 2010; Hochman, 2012; Raimondo et al., 2015). During neonatal seizures, there is an increase in neuronal volume and $[Cl^-]_i$ (Glykys et al., 2009, 2014a). A rise in $[Cl^-]_i$ is also observed in cytotoxic edema which can be prevented by decreasing the extracellular Cl^- concentration (Dijkstra et al., 2016; Rungta et al., 2015; Steffensen et al., 2015). Clinically, cytotoxic edema is observed in neonatal hypoxic-ischemic encephalopathy (HIE) and severe traumatic brain injury in humans, both of which are associated with seizures (Gutierrez et al., 2010; Nedelcu et al., 1999; Olsson et al., 2006; Unterberg et al., 2004; Wei et al., 2012). Finally, neurons from patients with mesial temporal epilepsy also demonstrate cytotoxic edema and increased $[Cl^-]_i$ (Huberfeld et al., 2007; Hufnagel et al., 2003; Szabo et al., 2005).

Modifying the extracellular osmolarity alters seizure activity

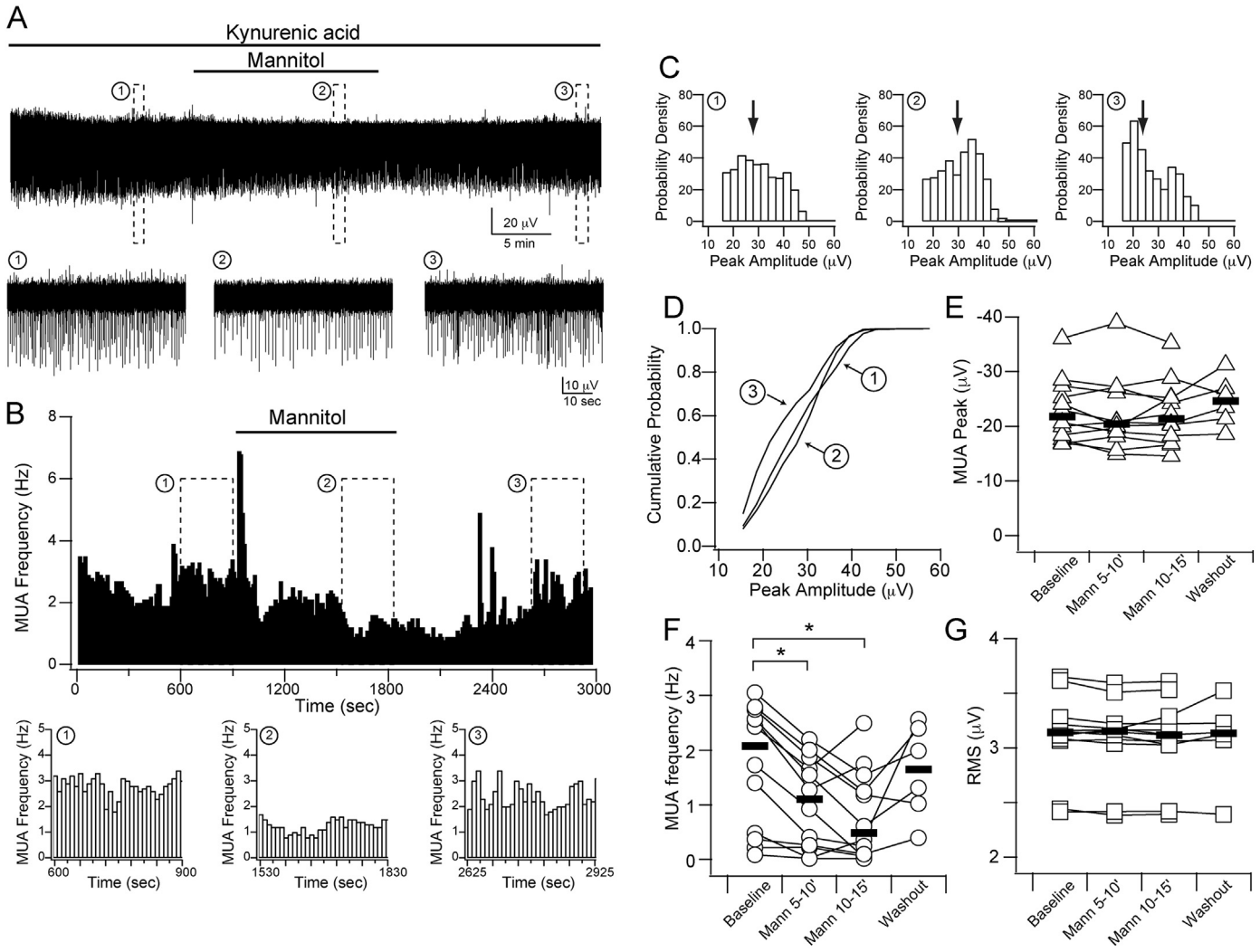

Fig. 5. Mannitol reduces spontaneous multiunit activity frequency but not amplitude. A) *Top,* Multiunit activity (MUA) recorded in the presence of 2 mM kynurenic acid and 50 μM 4-Aminopyridine (P8) and in the presence of mannitol (bottom line) in acute neocortical brain slices (Layer IV/V). *Below*, higher magnification of dashed boxes from baseline (1), under mannitol (2), and washout (3). B) *Top,* MUA frequency over time. *Below,* MUA frequency counts in the regions represented by the dashed boxes: baseline (1), mannitol (2), and washout (3). C) Peak amplitude probability density of detected events from the same segments depicted in B (Baseline: 27.9; Man: 29.6; Wash: 23.83 μV; median values). D) Cumulative distribution of peak amplitudes from segments in C. Note no change between control and mannitol perfusion. K-S test between all groups $p > .05$. E) MUA peak amplitudes are not different (P7–8) (open triangles: individual recordings; thick line: median; $n = 12$; $p = .472$, Friedman Repeated ANOVA on Ranks). F) MUA frequency decreases in the presence of mannitol (open circles: individual recordings; thick line: median; $n = 12$; $p < .001$; Friedman Repeated ANOVA on Ranks; *, Tukey post-hoc test $p < .05$). G) No change in baseline root mean square with mannitol ($p = .338$; Friedman Repeated ANOVA on ranks).

(Andrew, 1991) which points to its important role in this pathological condition. Hyperosmotic therapy with mannitol is one of the main treatments for elevated intracranial pressure which can be caused by severe cytotoxic and vascular edema (Carney et al., 2016). Mannitol creates a concentration gradient between the intravascular, interstitial, and intercellular compartments. It also improves cerebral perfusion pressure in hypoperfused brain regions, and alters blood viscosity (Muizelaar et al., 1983; Scalfani et al., 2012). Several mechanisms have been postulated to explain the actions of mannitol and other hypertonic solutions on epileptiform activity including changes in field effects (by increasing the extracellular space) and reducing excitatory post-synaptic potentials (Andrew et al., 1989; Andrew and MacVicar, 1994; Dudek et al., 1990; Hochman, 2012; Jefferys, 1995; Reed and Woodbury, 1964; Roper et al., 1992; Saly and Andrew, 1993; Traynelis and Dingledine, 1989).

Our results support a novel mechanism for mannitol, as prior studies did not address neuronal $[Cl^-]_i$. An increase in osmolarity by 20 mOsm induced by mannitol (similar to what is obtained with a clinical dose of 1 g/kg, Cloyd et al., 1985; Marshall et al., 1978; Polderman et al., 2003) decreases neuronal volume and $[Cl^-]_i$ (Fig. 3) which results in an enhancement of the inhibitory actions of GABA and of anticonvulsants that prolong the open time of $GABA_A$Rs such as benzodiazepines (Glykys et al., 2017). Therefore, our data argues against a pure field effect of mannitol in the neocortex during the neonatal period to explain its anticonvulsant effect. However, we do not negate that in areas with a higher neuronal density (*e.g. hippocampus*) or with significantly higher doses of mannitol than used in clinic, a change in field effect might become an additional explanation of the actions of mannitol on neuronal excitability. Our *in vitro* results support prior studies which demonstrated that intravascular mannitol decreases seizure-like activity in murine species as well as humans (Baran et al., 1987; Haglund and Hochman, 2005).

4.1.2. Neuronal Cl^- homeostasis and seizure control

Low $[Cl^-]_i$ is paramount for the inhibitory actions of GABA. A small increase in $[Cl^-]_i$ can alter GABA actions from hyperpolarization to

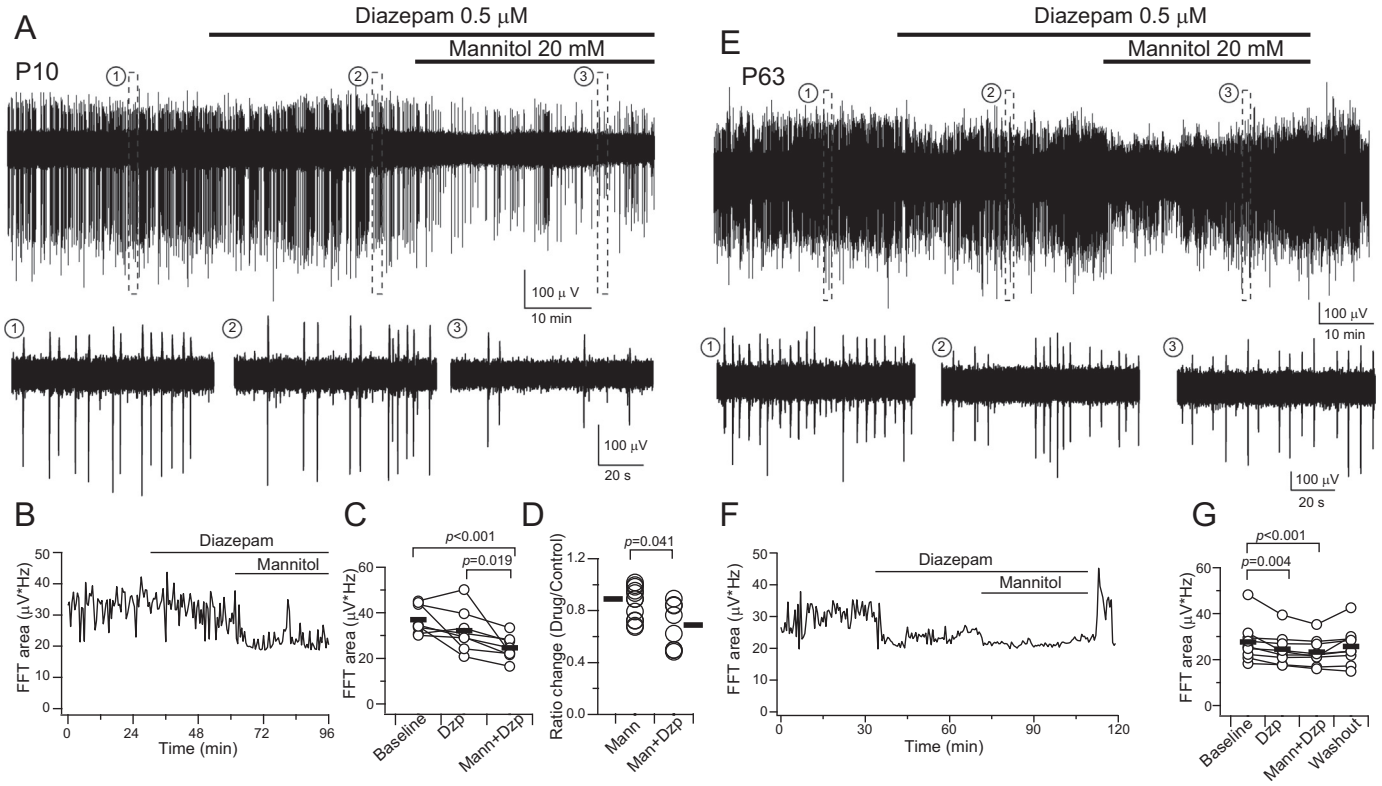

Fig. 6. A decrease in neuronal $[Cl^-]_i$ by mannitol potentiates the effect of benzodiazepines during early neocortical development. A) *Top, in vitro* epileptiform activity induced by Low-Mg^{2+} in the presence of diazepam (Dzp) and mannitol plus diazepam (Mann + Dzp) at P10 (acute brain slice, Layer IV/V). *Below*, higher magnification of areas: baseline (1), diazepam (2), and Mann + Dzp (3). B) FFT area from trace in A calculated every 30 s. C) Change in FFT area by the different drugs (thick line: mean; P10–11; $n = 8$; $p = .03$, ANOVA; Holm-Sidak post-hoc test). D) Ratio change between mannitol alone and Mann + Dzp (open circles: individual recordings; line: median). E) Same as A but recorded in an adult neocortical brain slice (P63). F) FFT area from trace in E calculated every 30 s. G) Change in FFT area by the different drugs (thick line: mean, P31–63; $n = 9$; $p = .001$, ANOVA; Holm-Sidak post-hoc test; percentage decrease between 2 and 25% for Dzp + Man).

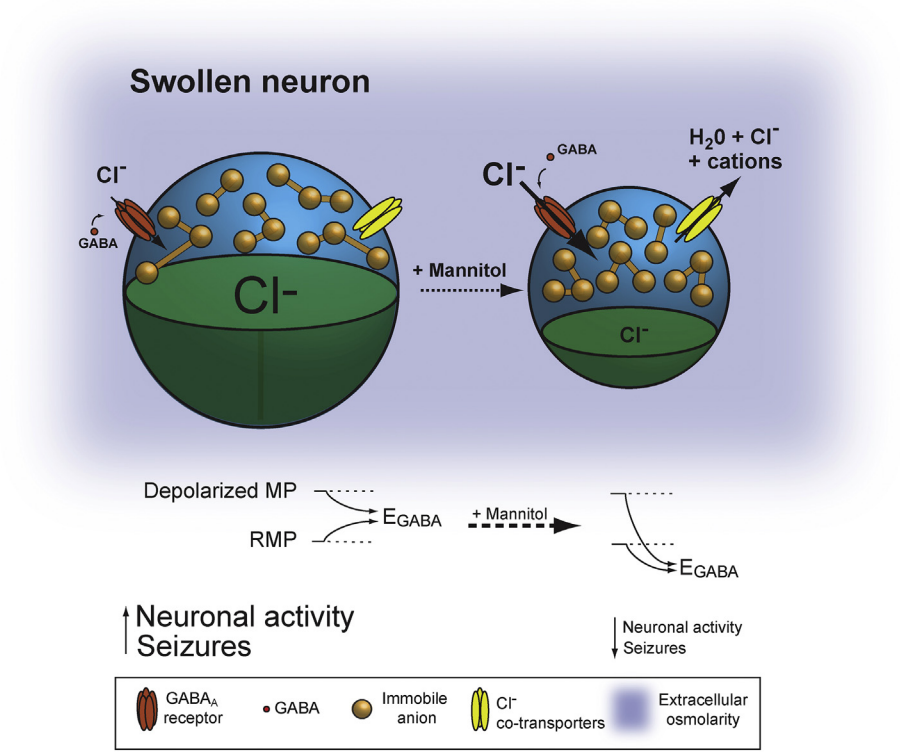

Fig. 7. Mannitol decreases neuronal $[Cl^-]_i$ and volume leading to improved inhibitory actions of GABA. An increase in extracellular osmolarity by mannitol leads to a decrease in neuronal $[Cl^-]_i$ and volume in neurons experiencing injury or seizures through CCCs (Figs. 3, 4). The decrease in $[Cl^-]_i$ leads to an increase GABAergic driving force. Two scenarios are illustrated: a depolarized membrane potential (MP) during seizures and a resting membrane potential (RMP) when neurons are not depolarized, with neurons having a minimal leak conductance for Cl^- (Chamberlin and Dingledine 1988; Yelhekar et al., 2017). The increase in GABAergic driving force results in decreased action potential firing (Fig. 5) and seizure activity (Figs. 1, 2, 6). The darker background represents an increase in extracellular osmolarity mediated by mannitol.

depolarization (Doyon et al., 2016; Glykys et al., 2017). Therefore, neuronal $[Cl^-]_i$ needs to be closely regulated. Our data supports the hypothesis that CCCs are involved in the movement of Cl^-, cations, and water to restore the $[Cl^-]_i$ set point as well as neuronal volume (Delpire and Staley, 2014; Doyon et al., 2011; Glykys et al., 2014a; Hoffmann et al., 2009; Kahle et al., 2015). During seizure activity, the role of CCCs in neuronal Cl^- homeostasis is particularly important due to the elevated levels of synaptic activity that can lead to an excess entry of Cl^-, cations and water (Glykys et al., 2009, 2014a; Raimondo et al., 2015).

Modulating neuronal $[Cl^-]_i$ is an important therapeutic strategy for the treatment of seizures. Blocking NKCC1, a conduit for Cl^- accumulation during seizures (Dzhala et al., 2010), increases the efficacy of $GABA_A$Rs positive allosteric modulators *in vitro* and *in vivo* (Dzhala et al., 2005; Erker et al., 2016; Glykys et al., 2009; Mazarati et al., 2009; Sivakumaran and Maguire, 2016). A small, uncontrolled human trial did not support this concept. However, this trial was not designed to test efficacy and the results are controversial (Pressler et al., 2015; Thoresen and Sabir, 2015). A controlled clinical trial has just completed their recruitment (NCT00830531, results pending), and the development of new NKCC1 blockers with better blood-brain permeability is underway (Töllner et al., 2014). Enhancing the activity of K^+-Cl^- co-transporter KCC2 (canonical exporter of Cl^-) is an additional proposed treatment for seizures by decreasing pathologically elevated $[Cl^-]_i$ (Friedel et al., 2015; Moore et al., 2017; Silayeva et al., 2015).

Here we provide an alternate approach: altering the extracellular osmolarity to simultaneously decrease neuronal $[Cl^-]_i$ and volume (Glykys et al., 2017). Neurons are unique in that volume and $[Cl^-]_i$ regulation are directly tied to the polarity of GABA actions, and there is a correlation between cytotoxic edema, Cl^- and seizures (Glykys et al., 2017). There is strong evidence of Cl^-, cations, and water being co-transported through CCCs (Gauvain et al., 2011; Hamann et al., 2010; Jourdain et al., 2011; MacAulay and Zeuthen, 2010; Zeuthen, 1994a; Zeuthen and Macaulay, 2012) since neurons do not have aquaporins and hence, a poor membrane water permeability (Aitken et al., 1998; Andrew et al., 2007; Lang et al., 1998) compared to epithelial cells, artificial membranes and astrocytes (Fettiplace and Haydon, 1980; Risher et al., 2009). The transport of Cl^- by NKCC1 and KCCs is coupled with a significant movement of water (MacAulay et al., 2004). KCCs and NKCC1 roughly transport 500 and 600 water molecules per cycle of ion movement respectively (Zeuthen, 1994b, 1994a; Zeuthen and Macaulay, 2012). Our results support the notion of the linked movement of water and Cl^- out of neurons, as when CCCs were blocked with furosemide, mannitol produced an increase in $[Cl^-]_i$ while continuing to decrease neuronal volume (Fig. 4) similarly to what we observed in organotypic hippocampal slices in the past (Glykys et al., 2014a). Whether the movement of Cl^- and water is through KCCs and/or the reversal of NKCC1 pump direction is beyond this study and will require further research.

4.1.3. Strengths and limitations

Strengths of our study include the use of a clinically relevant dose of mannitol and diazepam, as well as the use of two distinct models of epileptiform activity: the Low-Mg^{2+} model in acute brain slices and the neocortical organotypic slice culture model which has spontaneous epileptiform activity. An additional strength includes the use of electrophysiology as well as 2-photon fluorescence microscopy to obtain complimentary data regarding the neuronal effects of osmotic manipulations. This dual approach robustly compensates for the limitations of either technique; for example, the use of a slightly pH-sensitive fluorophore, Clomeleon, to study $[Cl^-]_i$ (Kuner and Augustine, 2000).

A limitation of this study is the use of *in vitro* models which permit the application of osmotic agents directly into the intercellular space rather than the intravascular space. Currently, it is unclear how an increase in intravascular space osmolarity alters intercellular space osmolarity. An intact blood brain barrier, as seen in the early post-injury phase when cytotoxic edema is predominant (Liang et al., 2007), would limit the flux of therapeutic osmolytes (either mannitol or NaCl) from the vascular to the intercellular space. In this circumstance, the effect of hyperosmolar therapy in the extracellular space would be the loss of free water and a concomitant increase in the intercellular NaCl concentration, more closely resembling our experiments with the perfusion of NaCl rather than the administration of mannitol. However, HIE status epilepticus and seizures are known to disrupt the blood-brain-barrier leading to vasogenic edema (Gutierrez et al., 2010; Kim et al., 2001; Rumpel et al., 1995). After the blood-brain barrier breaks down, mannitol and NaCl administered in the intravascular space may become distributed throughout the intercellular space. Under these conditions, a differential effect of mannitol and NaCl on epileptiform activity could be observed, as in our experiments. Interestingly, a dose of mannitol resulted in a decrease in epileptiform activity in human patients (Haglund and Hochman, 2005). The effects of mannitol observed in our experiments were modest but significant. Whether a clinically meaningful anticonvulsant effect of hyperosmolar therapy occurs will require a clinical correlation of electrographic seizure activity after hypertonic therapy at sequential times post-injury. Also, we concentrated our studies on the effect of mannitol during epileptiform activity. How healthy neurons activate regulatory volume increase (RVI) and decrease (RVD) mechanisms (Hoffmann et al., 2009) in response to altered extracellular osmolarity is of great interest, but beyond the scope of our current study. Lastly, we concentrated our studies in neurons, yet all central nervous cell types suffer cytotoxic edema. Astrocytes, in particular, swell during brain injury (Liang et al., 2007). Further studies are needed to determine how astrocytic Cl^- and its cell volume change in the presence of mannitol.

In conclusion, our results strongly support the hypothesis that an increase in extracellular osmolarity leads to the linked movement of Cl^- and water out of neurons. While we have focused on CCCs, there are alternate and redundant pathways that mediate the outward movement of water and Cl^- including the volume-regulated anion channel (VRAC) and other Cl^- channels (Hoffmann et al., 2009; Lambert et al., 2008; Pedersen et al., 2016; Qiu et al., 2014; Voss et al., 2014; Zeuthen, 2010) as it is suggested by the decrease in neuronal volume in the presence of mannitol when CCCs were blocked (Fig. 4) as well as our prior results (Glykys et al., 2014a).

A better understanding of volume and salt regulation, specifically in neurons, will lead to the development of new medical compounds that will not only improve neuronal cytotoxic edema but may lead to improved anticonvulsive treatments.

Supplementary data to this article can be found online at https://doi.org/10.1016/j.nbd.2019.01.024.

Conflict of interest

The authors declare no competing financial interests.

Acknowledgments

JG was supported by the NIH/NINDS 1K08NS091248 and through the support of the Iowa Neuroscience Institute. KS was supported by NIH/NINDS 5R01NS40109-14.

References

Aitken, P.G., Borgdorff, A.J., Juta, A.J.A., Kiehart, D.P., Somjen, G.G., Wadman, W.J., 1998. Volume changes induced by osmotic stress in freshly isolated rat hippocampal neurons. Pflugers Arch. J. Physiol. 436, 991–998. https://doi.org/10.1007/s004240050734.

Allen, N.J., Rossi, D.J., Attwell, D., 2004. Sequential release of GABA by exocytosis and reversed uptake leads to neuronal swelling in simulated ischemia of hippocampal slices. J. Neurosci. 24, 3837–3849. https://doi.org/10.1523/JNEUROSCI.5539-03.2004.

Amiry-Moghaddam, M., Ottersen, O.P., 2003. The molecular basis of water transport in the brain. Nat. Rev. Neurosci. 4, 991–1001. https://doi.org/10.1038/nrn1252.

Anderson, G., Miller, J., 2002. Benzodiazepines. Chemistry, biotransformation and

pharmacokinetics. In: Levy, R., Meldrum, B., Mattson, R., Perucca, E. (Eds.), Antiepileptic Drugs. LWW, Philadelphia, pp. 187–205.
Andrew, R.D., 1991. Seizure and acute osmotic change: clinical and neurophysiological aspects. J. Neurol. Sci. 101, 7–18. https://doi.org/10.1016/0022-510X(91)90013-W.
Andrew, R.D., MacVicar, B.A., 1994. Imaging cell volume changes and neuronal excitation in the hippocampal slice. Neuroscience 62, 371–383.
Andrew, R.D., Fagan, M., Ballyk, B.A., Rosen, A.S., 1989. Seizure susceptibility and the osmotic state. Brain Res. 498, 175–180. https://doi.org/10.1016/0006-8993(89)90417-4.
Andrew, R.D., Labron, M.W., Boehnke, S.E., Carnduff, L., Kirov, S.A., 2007. Physiological evidence that pyramidal neurons lack functional water channels. Cereb. Cortex 17, 787–802. https://doi.org/10.1093/cercor/bhk032.
Baran, H., Lassmann, H., Sperk, G., Seitelberger, F., Hornykiewicz, O., 1987. Effect of mannitol treatment on brain neurotransmitter markers in kainic acid-induced epilepsy. Neuroscience 21, 679–684. https://doi.org/10.1016/0306-4522(87)90029-7.
Bekkers, J.M., Stevens, C.F., 1996. Cable properties of cultured hippocampal neurons determined from sucrose-evoked miniature EPSCs. J. Neurophysiol. 75, 1250–1255. https://doi.org/10.1152/jn.1996.75.3.1250.
Ben-Ari, Y., 2002. Excitatory actions of gaba during development: the nature of the nurture. Nat. Rev. Neurosci. 3, 728–739. https://doi.org/10.1038/nrn920.
Ben-Ari, Y., Gaiarsa, J.-L., Tyzio, R., Khazipov, R., 2007. GABA: a pioneer transmitter that excites immature neurons and generates primitive oscillations. Physiol. Rev. 87, 1215–1284. https://doi.org/10.1152/physrev.00017.2006.
Blauwblomme, T., Dzhala, V., Staley, K., 2018. Transient ischemia facilitates neuronal chloride accumulation and severity of seizures. Ann. Clin. Transl. Neurol. 1–14. https://doi.org/10.1002/acn3.617.
Bormann, J., Hamill, O., Sakmann, B., 1987. Mechanism of anion permeation through channels gated by glycine and gamma-aminobutyric acid in mouse cultured spinal neurones. J. Physiol. 385, 243–286.
Bratton, S.L., Chestnut, R.M., Ghajar, J., McConnell Hammond, F.F., Harris, O. a, Hartl, R., Manley, G.T., Nemecek, A., Newell, D.W., Rosenthal, G., Schouten, J., Shutter, L., Timmons, S.D., Ullman, J.S., Videtta, W., Wilberger, J.E., Wright, D.W., 2007. Guidelines for the management of severe traumatic brain injury. II. Hyperosmolar therapy. J. Neurotrauma 24 (Suppl. 1), S14–S20. https://doi.org/10.1089/neu.2007.9994.
Carney, N., Totten, A.M., O'Reilly, C., Ullman, J.S., Hawryluk, G.W.J., Bell, M.J., Bratton, S.L., Chesnut, R., Harris, O.A., Kissoon, N., Rubiano, A.M., Shutter, L., Tasker, R.C., Vavilala, M.S., Wilberger, J., Wright, D.W., Ghajar, J., 2016. Guidelines for the management of severe traumatic brain injury, fourth edition. Neurosurgery 80, 6–15. https://doi.org/10.1227/NEU.0000000000001432.
Caspi, A., Benninger, F., Yaari, Y., 2009. KV7/M channels mediate osmotic modulation of intrinsic neuronal excitability. J. Neurosci. 29, 11098–11111. https://doi.org/10.1523/JNEUROSCI.0942-09.2009.
Chamberlin, N.L., Dingledine, R., 1988. GABAergic inhibition and the induction of spontaneous epileptiform activity by low chloride and high potassium in the hippocampal slice. Brain Res 445, 12–18. 10.1016/0006-8993(88)91068-2.
Cloyd, J., Snyder, B., Cleeremans, B., Cloyd, C., Bundlie, A., 1985. Mannitol pharmacokinetics and serum osmolality in dogs and humans. J. Pharmacol. Exp. Ther. 236, 301–306.
Connell, J., Oozeer, R., de Vries, L., Dubowitz, L.M., Dubowitz, V., 1989. Clinical and EEG response to anticonvulsants in neonatal seizures. Arch. Dis. Child. 64, 459–464. https://doi.org/10.1136/adc.64.4_Spec_No.459.
Deeb, T.Z., Nakamura, Y., Frost, G.D., Davies, P.A., Moss, S.J., 2013. Disrupted Cl-homeostasis contributes to reductions in the inhibitory efficacy of diazepam during hyperexcited states. Eur. J. Neurosci. 38, 2453–2467. https://doi.org/10.1111/ejn.12241.
Delpire, E., Staley, K., 2014. Novel determinants of the neuronal Cl- concentration. J. Physiol. 592, 4099–4114. https://doi.org/10.1113/jphysiol.2014.275529.
Dietzel, I., Heinemann, U., Hofmeier, G., Lux, H., 1980. Transient changes in the size of the extracellular space in the sensorimotor cortex of cats in relation to stimulus-induced changes in potassium concentration. Exp. Brain Res. 40, 432–439.
Dietzel, I., Heinemann, U., Hofmeier, G., Lux, H.D., 1982. Stimulus-induced changes in extracellular Na+ and Cl- concentration in relation to changes in the size of the extracellular space. Exp. Brain Res. 46, 73–84. https://doi.org/10.1007/BF00238100.
Dietzel, I., Heinemann, U., Lux, H.D., 1989. Relations between slow extracellular potential changes, glial potassium buffering, and electrolyte and cellular volume changes during neuronal hyperactivity in cat brain. Glia 2, 25–44. https://doi.org/10.1002/glia.440020104.
Dijkstra, K., Hofmeijer, J., van Gils, S., van Putten, M.J.A.M., 2016. A biophysical model for cytotoxic cell swelling. J. Neurosci. 36, 11881–11890. https://doi.org/10.1523/JNEUROSCI.1934-16.2016.
Doyon, N., Prescott, S.A., Castonguay, A., Godin, A.G., Kröger, H., de Koninck, Y., 2011. Efficacy of synaptic inhibition depends on multiple, dynamically interacting mechanisms implicated in chloride homeostasis. PLoS Comput. Biol. 7, e1002149. https://doi.org/10.1371/journal.pcbi.1002149.
Doyon, N., Vinay, L., Prescott, S.A.A., De Koninck, Y., De Koninck, Y., 2016. Chloride regulation: a dynamic equilibrium crucial for synaptic inhibition. Neuron 89, 1157–1172. https://doi.org/10.1016/j.neuron.2016.02.030.
Dudek, F.E., Obenaus, A., Tasker, J.G., 1990. Osmolality-induced changes in extracellular volume alter epileptiform bursts independent of chemical synapses in the rat: importance of non-synaptic mechanisms in hippocampal epileptogenesis. Neurosci. Lett. 120, 267–270.
Dzhala, V.I., Talos, D.M., Sdrulla, D.A., Brumback, A.C., Mathews, G.C., Benke, T.A., Delpire, E., Jensen, F.E., Staley, K.J., 2005. NKCC1 transporter facilitates seizures in the developing brain. Nat. Med. 11, 1205–1213. https://doi.org/10.1038/nm1301.
Dzhala, V.I., Kuchibhotla, K.V., Glykys, J.C., Kahle, K.T., Swiercz, W.B., Feng, G., Kuner, T., Augustine, G.J., Bacskai, B.J., Staley, K.J., 2010. Progressive NKCC1-dependent neuronal chloride accumulation during neonatal seizures. J. Neurosci. 30, 11745–11761. https://doi.org/10.1523/JNEUROSCI.1769-10.2010.
Dzhala, V., Valeeva, G., Glykys, J., Khazipov, R., Staley, K., 2012. Traumatic alterations in GABA signaling disrupt hippocampal network activity in the developing brain. J. Neurosci. 32. https://doi.org/10.1523/JNEUROSCI.5139-11.2012.
Erker, T., Brandt, C., Töllner, K., Schreppel, P., Twele, F., Schidlitzki, A., Löscher, W., 2016. The bumetanide prodrug BUM5, but not bumetanide, potentiates the anti-seizure effect of phenobarbital in adult epileptic mice. Epilepsia 57, 698–705. https://doi.org/10.1111/epi.13346.
Fettiplace, R., Haydon, D.A., 1980. Water Permeability of Lipid Membranes. vol. 60. pp. 510–550.
Friedel, P., Kahle, K.T., Zhang, J., Hertz, N., Pisella, L.I., Buhler, E., Schaller, F., Duan, J., Khanna, A.R., Bishop, P.N., Shokat, K.M., Medina, I., 2015. WNK1-regulated inhibitory phosphorylation of the KCC2 cotransporter maintains the depolarizing action of GABA in immature neurons. Sci. Signal. 8https://doi.org/10.1126/scisignal.aaa0354. (ra65).
Gauvain, G., Chamma, I., Chevy, Q., Cabezas, C., Irinopoulou, T., Bodrug, N., Carnaud, M., Levi, S., Poncer, J.C., 2011. The neuronal K-Cl cotransporter KCC2 influences postsynaptic AMPA receptor content and lateral diffusion in dendritic spines. Proc. Natl. Acad. Sci. 108, 15474–15479. https://doi.org/10.1073/pnas.1107893108.
Glass, H.C., 2014. Neonatal seizures. Advances in mechanisms and management. Clin. Perinatol. 41, 177–190. https://doi.org/10.1016/j.clp.2013.10.004.
Glykys, J., Staley, K.J., 2015. Diazepam effect during early neonatal development correlates with neuronal Cl^{-1}. Ann. Clin. Transl. Neurol. 2, 1055–1070. https://doi.org/10.1002/acn3.259.
Glykys, J., Staley, K.J., 2016. Developmental decrease of neuronal chloride concentration is independent of trauma in thalamocortical brain slices. PLoS One 11, e0158012. https://doi.org/10.1371/journal.pone.0158012.
Glykys, J., Dzhala, V.I., Kuchibhotla, K.V., Feng, G., Kuner, T., Augustine, G., Bacskai, B.J., Staley, K.J., 2009. Differences in cortical versus subcortical GABAergic signaling: a candidate mechanism of electroclinical uncoupling of neonatal seizures. Neuron 63, 657–672. https://doi.org/10.1016/j.neuron.2009.08.022.
Glykys, J., Dzhala, V., Egawa, K., Balena, T., Saponjian, Y., Kuchibhotla, K., Bacskai, B., Kahle, K., Zeuthen, T., Staley, K.J., 2014a. Local impermeant anions establish the neuronal chloride concentration. Science 343, 670–675. https://doi.org/10.1126/science.1245423.
Glykys, J., Dzhala, V., Egawa, T., Balena, T., Saponjian, Y., Kuchibhotla, K., Bacskai, B., Kahle, K., Zeuthen, T., Staley, K., 2014b. Response to comments on "local impermeant anions establish the neuronal chloride concentration". Science 345, 1130. https://doi.org/10.1126/science.1255337.
Glykys, J., Dzhala, V., Egawa, K., Kahle, K.T., Delpire, E., Staley, K., 2017. Chloride dysregulation, seizures, and cerebral edema: a relationship with therapeutic potential. Trends Neurosci. 40, 276–294. https://doi.org/10.1016/j.tins.2017.03.006.
Greenblatt, D.J., Sethy, V.H., 1990. Benzodiazepine concentrations in brain directly reflect receptor occupancy: studies of diazepam, lorazepam, and oxazepam. Psychopharmacology (Berl.) 102, 373–378. https://doi.org/10.1007/BF02244106.
Gutierrez, L.G., Rovira, À., Portela, L.A.P., Da Costa Leite, C., Lucato, L.T., 2010. CT and MR in non-neonatal hypoxic-ischemic encephalopathy: Radiological findings with pathophysiological correlations. Neuroradiology 52, 949–976. https://doi.org/10.1007/s00234-010-0728-z.
Haglund, M.M., Hochman, D.W., 2005. Furosemide and mannitol suppression of epileptic activity in the human brain. J. Neurophysiol. 94, 907–918. https://doi.org/10.1152/jn.00944.2004.
Hamann, S., Herrera-Perez, J.J., Zeuthen, T., Alvarez-Leefmans, F.J., 2010. Cotransport of water by the Na+-K+-2Cl(−) cotransporter NKCC1 in mammalian epithelial cells. J. Physiol. 588, 4089–4101. https://doi.org/10.1113/jphysiol.2010.194738.
Hochman, D.W., 2012. The extracellular space and epileptic activity in the adult brain: explaining the antiepileptic effects of furosemide and bumetanide. Epilepsia 53, 18–25. https://doi.org/10.1111/j.1528-1167.2012.03471.x.
Hoffmann, E., Lambert, I., Pedersen, S., 2009. Physiology of cell volume regulation in vertebrates. Physiol. Rev. 89, 193–277. https://doi.org/10.1152/physrev.00037.2007.
Huberfeld, G., Wittner, L., Clemenceau, S., Baulac, M., Kaila, K., Miles, R., Rivera, C., 2007. Perturbed chloride homeostasis and GABAergic signaling in human temporal lobe epilepsy. J. Neurosci. 27, 9866–9873. https://doi.org/10.1523/JNEUROSCI.2761-07.2007.
Hufnagel, A., Marks, S., Ludwig, T., De Greiff, A., Leonhardt, G., Widmann, G., Stolke, D., Forsting, M., 2003. Brain diffusion after single seizures. Epilepsia 44, 54–63.
Jefferys, J.G.R., 1995. Nonsynaptic modulation of neuronal-activity in the brain - electric currents and extracellular ions. Physiol. Rev. 75, 689–723.
Jourdain, P., Pavillon, N., Moratal, C., Boss, D., Rappaz, B., Depeursinge, C., Marquet, P., Magistretti, P.J., 2011. Determination of transmembrane water fluxes in neurons elicited by glutamate ionotropic receptors and by the cotransporters KCC2 and NKCC1: a digital holographic microscopy study. J. Neurosci. 31, 11846–11854. https://doi.org/10.1523/JNEUROSCI.0286-11.2011.
Kahle, K.T., Khanna, A.R., Alper, S.L., Adragna, N.C., Lauf, P.K., Sun, D., Delpire, E., 2015. K-Cl cotransporters, cell volume homeostasis, and neurological disease. Trends Mol. Med. 1, 1–11. https://doi.org/10.1016/j.molmed.2015.05.008.
Kim, J.A., Chung, J., Yoon, Pyeong Ho, Kim, Dong Ik, Chung, T.S., Kim, E.J., Jeong, E.K., 2001. Transient MR signal changes in patients with generalized tonicoclonic seizure or status epilepticus: periictal diffusion-weighted imaging. Am. J. Neuroradiol. 22, 1149–1160.
Kirmse, K., Kummer, M., Kovalchuk, Y., Witte, O.W., Garaschuk, O., Holthoff, K., 2015. GABA depolarizes immature neurons and inhibits network activity in the neonatal

neocortex in vivo. Nat. Commun. 6, 7750. https://doi.org/10.1038/ncomms8750.
Kuner, T., Augustine, G.J., 2000. A genetically encoded ratiometric indicator for chloride: capturing chloride transients in cultured hippocampal neurons. Neuron 27, 447–459. https://doi.org/10.1016/S0896-6273(00)00056-8.
Lambert, I.H., Hoffmann, E.K., Pedersen, S.F., 2008. Cell volume regulation: physiology and pathophysiology. Acta Physiol. (Oxf.) 194, 255–282. https://doi.org/10.1111/j.1748-1716.2008.01910.x.
Lang, F., Busch, G.L., Ritter, M., Vo, H., Waldegger, S., Gulbins, E., 1998. Functional significance of cell volume regulatory mechanisms. Physiol. Rev. 78, 247–307.
Lerma, J., Martin del, R.R., 1992. Chloride transport blockers prevent N-methyl-D-aspartate receptor-channel complex activation. Mol. Pharmacol. 41, 217–222.
Liang, D., Bhatta, S., Volodymyr, G., Simard, J.M., 2007. Cytotoxic edema: mechanisms of pathological cell swelling. Neurosurg. Focus. 22, 1–9. https://doi.org/10.3171/foc.2007.22.5.3.
Luhmann, H.J., Kirischuk, S., Kilb, W., 2014. Comment on “local impermeant anions establish the neuronal chloride concentration”. Science 345, 1130. https://doi.org/10.1126/science.1255337.
MacAulay, N., Zeuthen, T., 2010. Water transport between CNS compartments: contributions of aquaporins and cotransporters. Neuroscience 168, 941–956. https://doi.org/10.1016/j.neuroscience.2009.09.016.
MacAulay, N., Hamann, S., Zeuthen, T., 2004. Water transport in the brain: Role of cotransporters. Neuroscience 129, 1031–1044. https://doi.org/10.1016/j.neuroscience.2004.06.045.
Marshall, L.F., Smith, R.W., Rauscher, L. a, Shapiro, H.M., 1978. Mannitol dose requirements in brain-injured patients. J. Neurosurg. 48, 169–172. https://doi.org/10.3171/jns.1978.48.2.0169.
Mazarati, A., Shin, D., Sankar, R., 2009. Bumetanide inhibits rapid kindling in neonatal rats. Epilepsia 50, 2117–2122. https://doi.org/10.1111/j.1528-1167.2009.02048.x.
Mody, I., Lambert, J.D., Heinemann, U., 1987. Low extracellular magnesium induces epileptiform activity and spreading depression in rat hippocampal slices. J. Neurophysiol. 57, 869–888.
Moore, Y.E., Kelley, M.R., Brandon, N.J., Deeb, T.Z., Moss, S.J., 2017. Seizing control of KCC2: a new therapeutic target for epilepsy. Trends Neurosci. 40, 555–571. https://doi.org/10.1016/j.tins.2017.06.008.
Muizelaar, J.P., Wei, E.P., Kontos, H. a, Becker, D.P., 1983. Mannitol causes compensatory cerebral vasoconstriction and vasodilation in response to blood viscosity changes. J. Neurosurg. 59, 822–828. https://doi.org/10.3171/jns.1983.59.5.0822.
Nardou, R., Yamamoto, S., Bhar, A., Burnashev, N., Ben-Ari, Y., Khalilov, I., 2011a. Phenobarbital but not diazepam reduces AMPA/kainate receptor mediated currents and exerts opposite actions on initial seizures in the neonatal rat hippocampus. Front. Cell. Neurosci. 5, 16. https://doi.org/10.3389/fncel.2011.00016.
Nardou, R., Yamamoto, S., Chazal, G., Bhar, A., Ferrand, N., Dulac, O., Ben-Ari, Y., Khalilov, I., 2011b. Neuronal chloride accumulation and excitatory GABA underlie aggravation of neonatal epileptiform activities by phenobarbital. Brain 134, 987–1002. https://doi.org/10.1093/brain/awr041.
Nedelcu, J., Klein, M.A., Aguzzi, A., Boesiger, P., Martin, E., 1999. Biphasic edema after hypoxic-ischemic brain injury in neonatal rats reflects early neuronal and late glial damage. Pediatr. Res. 46, 297–304. https://doi.org/10.1203/00006450-199909000-00008.
Olsson, T., Broberg, M., Pope, K.J., Wallace, a., Mackenzie, L., Blomstrand, F., Nilsson, M., Willoughby, J.O., 2006. Cell swelling, seizures and spreading depression: an impedance study. Neuroscience 140, 505–515. https://doi.org/10.1016/j.neuroscience.2006.02.034.
Owens, D.F., Boyce, L.H., Davis, M.B., Kriegstein, A.R., 1996. Excitatory GABA responses in embryonic and neonatal cortical slices demonstrated by gramicidin perforated-patch recordings and calcium imaging. J. Neurosci. 16, 6414–6423.
Painter, M.J., Scher, M.S., Stein, A.D., Armatti, S., Wang, Z., Gardiner, J.C., Paneth, N., Minnigh, B., Alvin, J., 1999. Phenobarbital compared with phenytoin for the treatment of neonatal seizures. N. Engl. J. Med. 341, 485–489. https://doi.org/10.1056/NEJM199908123410704.
Pallud, J., Van Quyen, M.L., Bielle, F., Pellegrino, C., Varlet, P., Labussiere, M., Cresto, N., Dieme, M., Baulac, M., Duyckaerts, C., Kourdougli, N., Chazal, G., Devaux, B., Rivera, C., Miles, R., Capelle, L., Huberfeld, G., 2014. Cortical GABAergic excitation contributes to epileptic activities around human glioma. Sci. Transl. Med. 6, 244ra89.
Pedersen, S.F., Okada, Y., Nilius, B., 2016. Biophysics and physiology of the volume-regulated anion channel (VRAC)/volume-sensitive outwardly rectifying anion channel (VSOR). Pflugers Arch. Eur. J. Physiol. 468, 371–383. https://doi.org/10.1007/s00424-015-1781-6.
Pitfield, A., Carroll, A., Kissoon, N., 2012. Emergency management of increased intracranial pressure. Pediatr. Emerg. Care 28, 200–204.
Polderman, K.H., van de Kraats, G., Dixon, J.M., Vandertop, W.P., Girbes, A.R.J., 2003. Increases in spinal fluid osmolarity induced by mannitol. Crit. Care Med. 31, 584–590. https://doi.org/10.1097/01.CCM.0000050287.68977.84.
Pond, B.B., Berglund, K., Kuner, T., Feng, G., Augustine, G.J., Schwartz-Bloom, R.D., 2006. The chloride transporter Na(+)-K(+)-Cl- cotransporter isoform-1 contributes to intracellular chloride increases after in vitro ischemia. J. Neurosci. 26, 1396–1406. https://doi.org/10.1523/JNEUROSCI.1421-05.2006.
Pressler, R.M., Boylan, G.B., Marlow, N., Blennow, M., Chiron, C., Cross, J.H., de Vries, L.S., Hallberg, B., Hellström-Westas, L., Jullien, V., Livingstone, V., Mangum, B., Murphy, B., Murray, D., Pons, G., Rennie, J., Swarte, R., Toet, M.C., Vanhatalo, S., Zohar, S., 2015. Bumetanide for the treatment of seizures in newborn babies with hypoxic ischaemic encephalopathy (NEMO): an open-label, dose finding, and feasibility phase 1/2 trial. Lancet Neurol. 14, 469–477. https://doi.org/10.1016/S1474-4422(14)70303-5.
Qiu, Z., Dubin, A.E., Mathur, J., Tu, B., Reddy, K., Miraglia, L.J., Reinhardt, J., Orth, A.P., Patapoutian, A., 2014. SWELL1, a plasma membrane protein, is an essential component of volume-regulated anion channel. Cell 157, 447–458. https://doi.org/10.1016/j.cell.2014.03.024.
Raimondo, J.V., Burman, R.J., Katz, A.A., Akerman, C.J., 2015. Ion dynamics during seizures. Front. Cell. Neurosci. 9, 1–14. https://doi.org/10.3389/fncel.2015.00419.
Reed, D.J., Woodbury, D.M., 1964. The effect of hypertonic urea solution on electroshock seizure threshold and electrolyte distribution in rats. J. Pharmacol. Exp. Ther. 146, 154–159.
Rheims, S., Minlebaev, M., Ivanov, A., Represa, A., Khazipov, R., Holmes, G.L., Ben-ari, Y., Zilberter, Y., 2008. Excitatory GABA in Rodent developing Neocortex in Vitro. J. Neurophysiol. 100, 609–619. https://doi.org/10.1152/jn.90402.2008.
Risher, W.C., Andrew, R.D., Kirov, S.A., 2009. Real-time passive volume responses of astrocytes to acute osmotic and ischemic stress in cortical slices and in vivo revealed by two-photon microscopy. Glia 57, 207–221. https://doi.org/10.1002/glia.20747.
Roper, S.N., Obenaus, A., Dudek, F.E., 1992. Osmolality and nonsynaptic epileptiform bursts in rat CA1 and dentate gyrus. Ann. Neurol. 31, 81–85. https://doi.org/10.1002/ana.410310115.
Ropper, A.H., 2014. Management of raised intracranial pressure and hyperosmolar therapy. Pract. Neurol. 14, 152–158. https://doi.org/10.1136/practneurol-2014-000811.
Rumpel, H., Buchli, R., Gehrmann, J., Aguzzi, A., Illi, O., Martin, E., 1995. Magnetic resonance imaging of brain edema in the neonatal rat - a comparison of short and long term hypoxia-ischemia. Pediatr. Res. 38, 113–118. https://doi.org/10.1203/00006450-199507000-00020.
Rungta, R.L., Choi, H.B., Tyson, J.R., Malik, A., Dissing-Olesen, L., Lin, P.J.C., Cain, S.M., Cullis, P.R., Snutch, T.P., Macvicar, B.A., 2015. The cellular mechanisms of neuronal swelling underlying cytotoxic edema. Cell 161, 610–621. https://doi.org/10.1016/j.cell.2015.03.029.
Saly, V., Andrew, R., 1993. CA3 neuron excitation and epileptiform discharge are sensitive to osmolality. J. Neurophysiol. 69, 2200–2208.
Scalfani, M.T., Dhar, R., Zazulia, A.R., Videen, T.O., Diringer, M.N., 2012. Effect of osmotic agents on regional cerebral blood flow in traumatic brain injury. J. Crit. Care 27https://doi.org/10.1016/j.jcrc.2011.10.008. (526.e7-526.e12).
Silayeva, L., Deeb, T.Z., Hines, R.M., Kelley, M.R., Munoz, M.B., Lee, H.H.C., Brandon, N.J., Dunlop, J., Maguire, J., Davies, P.A., Moss, S.J., 2015. KCC2 activity is critical in limiting the onset and severity of status epilepticus. Proc. Natl. Acad. Sci. U. S. A. 112, 3523–3528. https://doi.org/10.1073/pnas.1415126112.
Sivakumaran, S., Maguire, J., 2016. Bumetanide reduces seizure progression and the development of pharmacoresistant status epilepticus. Epilepsia 57, 222–232. https://doi.org/10.1111/epi.13270.
Staley, K.J., Longacher, M., Bains, J.S., Yee, A., 1998. Presynaptic modulation of CA3 network activity. Nat. Neurosci. 1, 201–209. https://doi.org/10.1038/651.
Steffensen, A.B., Sword, J., Croom, D., Kirov, S.A., MacAulay, N., 2015. Chloride cotransporters as a molecular mechanism underlying spreading depolarization-induced dendritic beading. J. Neurosci. 35, 12172–12187. https://doi.org/10.1523/JNEUROSCI.0400-15.2015.
Stevens, C.F., Tsujimoto, T., 1995. Estimates for the pool size of releasable quanta at a single central synapse and for the time required to refill the pool. Proc. Natl. Acad. Sci. U. S. A. 92, 846–849. https://doi.org/10.1073/pnas.92.3.846.
Stevenson, N.J., Boylan, G.B., Hellström-Westas, L., Vanhatalo, S., 2016. Treatment trials for neonatal seizures: the effect of design on sample size. PLoS One 11, e0165693. https://doi.org/10.1371/journal.pone.0165693.
Sulis Sato, S., Artoni, P., Landi, S., Cozzolino, O., Parra, R., Pracucci, E., Trovato, F., Szczurkowska, J., Luin, S., Arosio, D., Beltram, F., Cancedda, L., Kaila, K., Ratto, G.M., 2017. Simultaneous two-photon imaging of intracellular chloride concentration and pH in the brain in vivo. Proc. Natl. Acad. Sci. 114, E8770–E8779. https://doi.org/10.1073/PNAS.1702861114.
Szabo, K., Poepel, A., Pohlmann-Eden, B., Hirsch, J., Back, T., Sedlaczek, O., Hennerici, M., Gass, A., 2005. Diffusion-weighted and perfusion MRI demonstrates parenchymal changes in complex partial status epilepticus. Brain 128, 1369–1376. https://doi.org/10.1093/brain/awh454.
Thoresen, M., Sabir, H., 2015. Epilepsy: Neonatal seizures still lack safe and effective treatment. Nat. Rev. Neurol. 11, 311–312. https://doi.org/10.1038/nrneurol.2015.74.
Töllner, K., Brandt, C., Töpfer, M., Brunhofer, G., Erker, T., Gabriel, M., Feit, P.W., Lindfors, J., Kaila, K., Löscher, W., 2014. A novel prodrug-based strategy to increase effects of bumetanide in epilepsy. Ann. Neurol. 75, 550–562. https://doi.org/10.1002/ana.24124.
Traynelis, S.F., Dingledine, R., 1989. Role of extracellular space in hyperosmotic suppression of potassium-induced electrographic seizures. J. Neurophysiol. 61, 927–938.
Unterberg, A., Stover, J., Kress, B., Kiening, K.L., 2004. Edema and brain trauma. Neuroscience 129, 1021–1029. https://doi.org/10.1016/j.neuroscience.2004.06.046.
Voipio, J., Boron, W., Jones, S., Hopfer, U., Payne, J., Kaila, K., 2014. Comment on “local impermeant anions establish the neuronal chloride concentration”. Science 345, 1130. https://doi.org/10.1126/science.1255337.
Voss, F.K., Ullrich, F., Münch, J., Lazarow, K., Lutter, D., Mah, N., Andrade-Navarro, M. a, von Kries, J.P., Stauber, T., Jentsch, T.J., 2014. Identification of LRRC8 heteromers as an essential component of the volume-regulated anion channel VRAC. Science 344, 634–638. https://doi.org/10.1126/science.1252826.
Wei, X.-E., Zhang, Y.-Z., Li, Y.-H., Li, M.-H., Li, W.-B., 2012. Dynamics of rabbit brain edema in focal lesion and perilesion area after traumatic brain injury: a MRI study. J. Neurotrauma 29, 2413–2420. https://doi.org/10.1089/neu.2010.1510.
Yelhekar, T.D., Druzin, M., Johansson, S., 2017. Contribution of Resting Conductance, GABA A-Receptor Mediated Miniature Synaptic Currents and Neurosteroid to Chloride Homeostasis in Central Neurons. Eneuro 4 (2). https://doi.org/10.1523/ENEURO.0019-17.2017.

Zeuthen, T., 1991. Water permeability of ventricular cell membrane in choroid plexus epithelium from Necturus maculosus. J. Physiol. 444, 133–151. https://doi.org/10.1113/jphysiol.1991.sp018871.
Zeuthen, T., 1994a. Cotransport of K+, Cl- and H20 by membrane proteins from choroid plexus epithelium of Necturus maculosus. J. Physiol. 478 (2), 203–219.
Zeuthen, T., 1994b. K+, CO- and H20 by membrane. Proteins 203–219.
Zeuthen, T., 2010. Water-transporting proteins. J. Membr. Biol. 234, 57–73. https://doi.org/10.1007/s00232-009-9216-y.
Zeuthen, T., Macaulay, N., 2012. Cotransport of water by Na^+-K^+-$2Cl^-$ cotransporters expressed in Xenopus oocytes: NKCC1 versus NKCC2. J. Physiol. 590, 1139–1154. https://doi.org/10.1113/jphysiol.2011.226316.